The influence of nutrients and light on the stoichiometry of ice algae and phytoplankton

Sander Verbiest

(3401863)

Supervisors: Eva Leu & Katja Philippart

Abstract

Organisms are made of elements such as carbon, nitrogen and phosphorus. The stoichiometric ratios between these elements are highly variable in primary producers and depend on nutrient and light availability. On a local scale, these stoichiometric ratios influence food quality and energy transfer within the food web. On a global scale they impact the carbon cycle. Understanding what drives variations in these ratios is therefore of major importance. Extensive fieldwork was performed on both sympagic as pelagic algal communities in van Mijenfjorden, Spitsbergen, during the spring and summer of 2017, in order to get a better understanding of what drives variations in stoichiometric ratios. Due to their different habitat, sympagic algae appeared to be more light adapted than phytoplankton.

Contents

Introduction

Arctic ecosystems are subject to extreme variations in light conditions, ranging from total darkness during the winter months to permanent daylight during the summer. During a large part of the year, there is insufficient light for algae to grow. After the winter solstice, the solar angle starts increasing gradually. It is only with the return of the light in spring that primary production starts again.

In ice covered systems, there are two main algal blooms during spring/early summer (Søreide, Leu et al. 2010). The first one occurs when ice algae growing within and attached to the bottom of the ice receive enough light to grow exponentially. The second bloom consists of phytoplankton and is also light induced. Although both the sympagic and the pelagic bloom depend on sufficiently high light levels to start, indirectly bloom initiation is controlled by a wide range of factors.

The start of the sympagic spring bloom in ice covered waters is light induced, but the available amount of photosynthetic active radiation (PAR) is not only determined by the solar angle, but also by the ice cover and more importantly, by the snow layer on top of the ice. Snow has a very high albedo of around 0.80 to 0.9, so most of the incoming light gets reflected immediately (Mundy, Gosselin et al. 2014), (Campbell, Mundy et al. 2016). Snow also has a high attenuation coefficient, further limiting the amount of light penetrating the snow and ice cover deep enough to reach the primary producers. Snow depth is not only dependent on precipitation, but also on the timing of ice formation, as an earlier ice formation allows snow to accumulate over a longer period of time. Locally, wind is can be an important player, as snow depths can vary substantially due to wind drifts (Mundy, Barber et al. 2005).

The development of sympagic algal communities depends on a range of additional factors. In order for a sympagic algal bloom to develop in spring, a seeding population has to be incorporated in the ice when it is formed. The timing of sea ice formation is an important factor governing the colonisation of sea ice (Niemi, Michel et al. 2011). After the summer production period, algal concentrations in the water steadily decline over fall and winter. Because of this, ice formation in late fall/early winter results in a higher concentration of ice algae in the ice awaiting the spring, as compared to sea ice formation in late winter, when algal concentrations in the water column are lower.

Another important factor that undergoes strong seasonal changes is nutrient availability. In wintertime, primary production is absent, so there is no drawdown of nutrients. At the same time, the remineralisation of organic matter increases the concentrations of nutrients in the water. Wintertime cooling of surface waters creates an inverted density gradient in the water column. The sinking of cold high density surface water eventually dissolves the stratification remnant of the summer (Eicken 1992). The absence of stratification in autumn and winter, combined with autumn and winter storms, enables vertical mixing of the water column down to the bottom. This is of major relevance to the nutrient resupply of the water column, as a large part of the remineralisation of organic matter occurs in the benthos (Michel, Legendre et al. 1996) and below the photic zone (Redfield 1958).

The algae forming the sympagic spring bloom are the first to start using the nutrient pool, albeit at a spatially very limited scale. The majority of the algae grow at the ice-water interface where there is nutrient exchange between the ice and the underlying water, but they are not capable of depleting the vast amount of nutrients in the water. Within the ice however, nutrient depletion does

occur. The greater the distance from the ice-water interface the less exchange there is, so higher up in the ice, nutrients become limiting faster than closer to the water. It is only at the peak of the sympagic bloom that the resupply of nutrients is not fast enough to match the algae's demand, resulting in nutrient limitation of the algae even in the bottom part of the sea ice (Michel, Ingram et al. 2006), especially when currents are weak (Cota, Prinsenberg et al. 1987).

Carbon limitation is also a real scenario as ice serves as lid preventing the exchange of carbon dioxide from the atmosphere with the water. Especially away from the ice-water interface, in dense algal communities, the demand for carbon can outweigh the supply (McMinn, Skerratt et al. 1999). Higher up in the ice, salinity can also become limiting to algal growth. As the salinity of the brine pockets in which the algae grow is inversely related to temperature, ice algae can subjected to high osmotic pressures (Eicken 1992). Below temperatures of -5.5 to -6 °C with matching salinities in excess of 90 to 100 PSU, ice algae stop growing (Kottmeier, Sullivan 1988), (Bartsch 1989), (Zhang, Gradinger et al. 1999). Other factors potentially influencing chlorophyll a biomass are species composition (Gosselin, Levasseur et al. 1997), (Finkel, Quigg et al. 2006) and the stability or the ice matrix (Campbell, Mundy et al. 2015). The relative importance of these factors differs between study areas and seasons (Leu, Mundy et al. 2015).

Sympagic blooms go through three stages (Leu, Mundy et al. 2015). In the first stage, light levels are not high enough to for bloom initiation and the ecosystem in the ice remains net heterotrophic. As the solar angle increases and the days get longer, the available photosynthetic radiation (PAR) passes the critical threshold for ice algae to grow exponentially, thus starting the bloom, phase two. Phase three occurs when ice temperatures rise to a level where the ice algae get disconnected from the ice by the flushing of widening brine channels and the melting of the sea ice from below. The majority of the algae released from the ice serve as a food source to the zooplankton community in the water, but because the of the shear amount of algae, combined with the suddenness of the release, a substantial part sediments down to the benthos and supports the community there (Michel, Legendre et al. 1996).

Just as the spring sympagic bloom, the pelagic spring bloom is light induced. Increased PAR levels in the water column can be the result of melting processes reducing the shading effect of ice and snow, giving rise to a pelagic under ice bloom (Arrigo, Perovich et al. 2012), (Mundy, Gosselin et al. 2014), or simply the result of ice breakup (Perrette, Yool et al. 2011). After the start of the pelagic bloom, pelagic nutrient concentrations quickly drop as the phytoplankton bloom develops. The melting of the sea ice, combined with increased runoff from the land both enhance the natural stratification that is the result from the increasing temperatures of the surface water ((Eicken 1992) and references therein). Especially in the surface mixed layer, this can lead to a rapid nutrient depletion, making the growing season for pelagic blooms rather short. During the bloom the plankton community is dominated by autotrophs, but later in the season this dominance is taken over by heterotrophs. Most of the autotrophic biomass is metabolised by secondary producers in the photic zone. This results in the freeing and release of nutrients into the water column, facilitating primary production after the initial spring bloom (Wassmann, Reigstad 2011).

The timing of sympagic and pelagic blooms are important determinants when it comes to the transfer of elements and energy to higher trophic levels. Grazers time their reproduction and growth to the sympagic and pelagic blooms respectively. The key Arctic grazer, the copepod *Calanus glacialis* uses the sympagic algal bloom to fuel egg production. The hatchlings in turn use the phytoplankton bloom for growth. Ice algae thus prolong the window for reproduction and growth for secondary producers (Leu, Søreide et al. 2011), (Søreide, Leu et al. 2010).

Organisms consist of elements such as carbon (C), nitrogen (N) and phosphorus (P). They acquire these nutrients from their surroundings, in the case of primary producers, or, in the case of grazers and predators, from dietary uptake. The stoichiometric ratios, i.e. the ratios between the different elements, differ from organism to organism. While stoichiometric ratios in primary producers are relatively flexible and dependent on environmental conditions, they are much more fixed in grazers and on higher trophic levels. The uptake of food with an elemental composition differing from the consumer's needs leads to a decreased efficiency in food uptake and growth. As a result, the stoichiometry of primary producers influences the species composition on higher trophic levels, which in turn has implications for the transfer of energy within the food web (Sterner, Elser 2002).

The Redfield ratio C:N:P of 106:16:1 (C:N = 6.6) (Redfield 1958) reflects the average stoichiometry of the global plankton community in the current environment (Arrigo 2004). Some empirical studies proposed different ratios, such as 166:20:1 (C:N = 8.3) for all seston (freshwater and marine) (Sterner, Andersen et al. 2008), or higher N:P ratios (Falkowski 2000) and references therein). A meta study including the Arctic shelves and ocean reported most values between the Redfield ratio and the one proposed by Sterner. The ratios from the waters around Svalbard were generally closer to the Redfield ratio, with C:N ratios for the Arctic Ocean of 6.6, the Greenland Sea of 6.9, the Atlantic influenced Barents Sea of 6.7 and the Arctic influenced Barents Sea of 7.9 (Frigstad, Andersen et al. 2014).

Nutrients and light are known to influence the stoichiometry of primary producers (Sterner, Elser 2002), (Galbraith, Martiny 2015), (Thrane, Hessen et al. 2016). Autotrophs have a much larger flexibility than secondary producers when it comes to elemental ratios. An excess of nutrients over what is directly needed for growth results in so called “luxury consumption”, the storage of nutrients in the vacuole or cytoplasm of an algal cell, lowering the C:N and C:P ratios. Vice versa, nutrient limitation results in increased carbon to nutrient ratios, as continued carbon fixation and subsequent storage dilutes other stoichiometric constituents. Similarly, available PAR can alter stoichiometric ratios because it is directly linked to carbon fixation and intracellular nutrient allocation (Sterner, Elser 2002).

Grazers generally have a higher demand for N and P than the autotrophs they feed on (Sterner, Elser 2002). As a result, high C:N and C:P ratios in primary producers have the potential to limit the growth of organisms higher up the food chain (Hessen, Leu et al. 2008). However, copepods can have a relatively high demand for carbon due to their build up of lipid stores (Daly, Wallace et al. 1999) and the higher C:N and C:P ratios encountered later in the season might actually be beneficial for lipid synthesis (Hessen, Leu et al. 2008). In contrast to the growth of the adult stages, the production and hatching success of copepod eggs is negatively correlated with high C:N ratios (Jónasdóttir, Gudfinnsson et al. 2002).

Hence, it is not only the amount of food available to consumers that affects their growth, but also the quality. At low light conditions, algal biomass tends to be low, but of good quality (i.e. low carbon to nutrient ratios). When there is a lot of light available for photosynthesis, the amount of algal biomass that can serve as a food source for grazers increases. However, the increase of primary producers causes a drawdown of nutrients. This can result in high algal biomass, but with a poor nutritional value. In this situation, consumers can experience a so called “paradox of enrichment”. Despite the abundance of food, they are still limited in their growth by the poor quality of their food. (Hessen, Leu et al. 2008).

In the Arctic, light conditions and nutrient availability are changing profoundly as a

consequence of the ongoing global warming. The Arctic sea ice extent has been decreasing progressively faster since the late seventies and when current green house gas emissions remain unchecked, an ice free Arctic during the summer is predicted to happen before the middle of this century (Perovich, Richter-Menge 2009), (Notz, Stroeve 2016). Between 1998 and 2009, the extent of open water increased by more than a quarter, and seasonally ice covered waters were on average one and a half month longer ice free (Arrigo, van Dijken 2011). At the same time, the ice that is present, is decreasing in thickness and has a greater area of melt ponds during the growth season, altering the light conditions for microalgae in sea ice and the underlying water (Arrigo, Perovich et al. 2012). On top of this, he sympagic community is experiencing earlier starts of the melting season, reducing the growing season for ice algae (Mundy, Gosselin et al. 2014).

Future changes in ice cover are also expected to influence nutrient concentrations, as an increase in melt processes will lead to a more stable and shallower stratification of the water column, limiting the vertical exchange of nutrients (Slagstad, Ellingsen et al. 2011). Potentially counteracting this effect of stratification in coastal zones, is an increased inflow of nutrients from the land, a result of the increased river discharge into the Arctic ocean as measured over the course of the past century (Peterson, Holmes et al. 2002). However, the extra sediment load that accompanies the increased river discharge also increases the turbidity of coastal waters, reducing the amount of light available to phytoplankton (Pabi, van Dijken et al. 2008).

Although climate change effects will differ from area to area, precipitation in large parts of the Arctic is expected to increase. Depending on whether this precipitation will fall as rain or snow, light penetration through the sea ice will either increase or decrease (Hartmann, Klein Tank et al. 2013).

Higher temperatures decrease the light attenuation of snow (Mundy, Barber et al. 2005). Given that sea ice starts to melt and break up earlier in the season, phytoplankton are expected to benefit from the increase PAR availability, especially early in the season (Arrigo 2013).

Due to the expected changes in nutrient and light availability, the average stoichiometry of the phytoplankton community is expected to change as well (Arrigo 2004).

In addition to long term changes, there is also a natural seasonal variability. Recent findings from the Canadian Arctic show that POC:PON ratios in sea ice algae vary over the course of a year (Niemi, Michel 2015).

From a climate modelling perspective, the Arctic waters are an important factor. Despite that they only account for 3 percent of the total area of the global oceans, they are responsible for 13 percent of the world's carbon uptake (Frigstad, Andersen et al. 2014). Thus, understanding the processes and factors behind the primary production in the Arctic is crucial in predicting future scenarios. The extreme seasonality of the Arctic makes it an ideal location for in situ research on the stoichiometric response of phytoplankton and ice algae to changing light and nutrient conditions.

The aim of this study is to get a better understanding of the importance of light and nutrients in governing seasonal changes in the stoichiometry of primary producers in a poorly studied area, and to reveal whether there are fundamental differences between sea ice algae and phytoplankton with respect to those dynamics.

Methods

Study area

The sampling for this project was conducted as part of the FAABulous project (FAABulous: Future Arctic Algal Blooms – and their role in the context of climate change) in van Mijenfjorden. Van Mijenfjorden is located on the western side of the island Spitsbergen, part of the Svalbard archipelago. The fjord is approximately ten kilometres wide and 50 kilometres long. The entrance of the fjord is largely closed off by an island, Akseløya. This limits the exchange of fjord water with the warm Atlantic water from the West Spitsbergen Current, and as a result, wintertime sea ice formation is favoured.

Samples for this study were taken from a total of 9 stations in van Mijenfjorden, Svalbard, between the 7th of January and the 14th of June 2017 (Figure 1) (for coordinates view Appendix A).

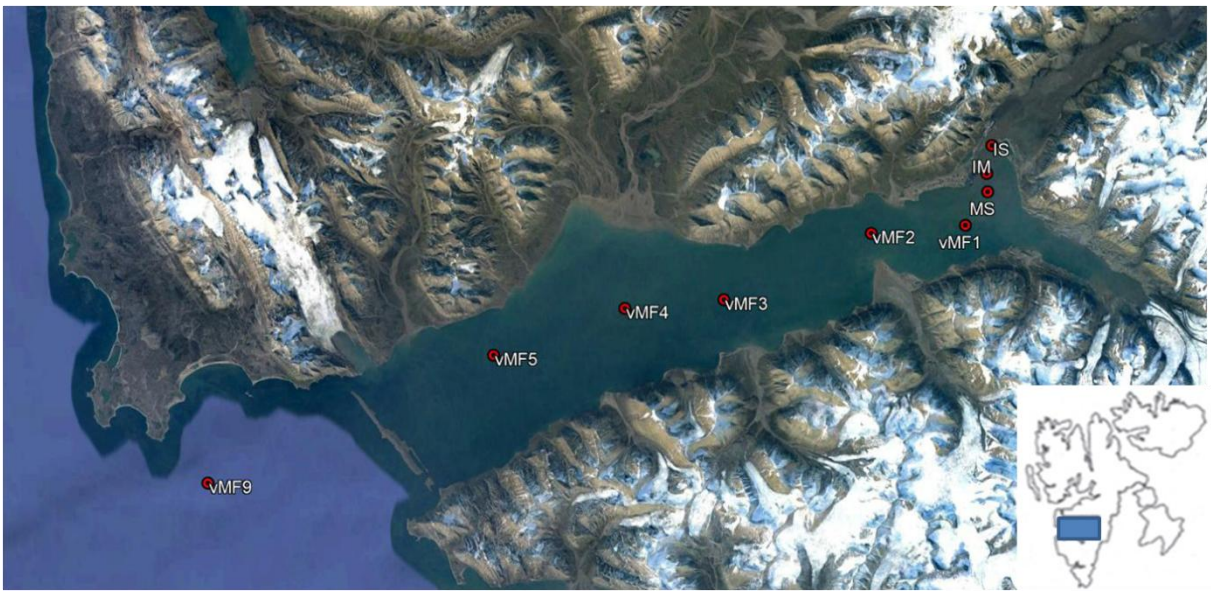

Figure 1. Map showing the locations of the stations sampled.

Sampling

Pelagic sampling was performed at seven different stations on 14 different days using a 10L Niskin bottle (Table 1). Depending on the ice conditions, sampling was either ice based or ship based. Depths sampled were 0m (ice based only) 5m, 15m, 25m, 50m (where applicable) and bottom.

Sympagic sampling was performed at five different stations on 11 different days (Table 1) using a Kovacs Mark2 ice corer with a diameter of 9cm. (Kovacs Enterprise, Roseburg, USA). On each sampling day, three sets of six cores each were taken approximately one meter apart. During the main field campaign in April/May, a high variability in snow depth was observed, being the result of wind drift. Snow depth is the main factor determining the adsorption of incoming solar irradiance. To compare the effect of the different snow depths on sympagic algae, on the 23rd and 26th of April and on the 2nd of May samples were taken from areas with low (0-5cm) snow and high (20+cm) snow cover.

Ice cores were protected from direct light and were cut into two sections; 0-3cm and 3-10cm, measured from the ice-water interface. Samples were left to thaw in the dark at 5-10 °C, after adding 100 ml of 0.7µm GF/F filtered sea water per cm of core to prevent osmotic shock. After thawing, the

volume of the samples was measured and sets of six samples were pooled in order to obtain three pools per core section and per treatment in the case of low versus high snow. For each pool, an additional core was sectioned and left to thaw without the addition of filtered seawater, to be used for nutrient analysis. An extra set of cores was measured for temperature, sectioned for salinity measurements and left to thaw without addition of filtered sea water.

From each water depth (pelagic) and core section (sympagic), water was filtered for chlorophyll a (Chla), particulate organic carbon and nitrogen (POC/PON) and particulate organic phosphorus (POP).

Table 1. General overview of sampling dates and stations for both pelagic and sympagic sampling. For locations of the stations, view Figure 1.

Date	Location pelagic	Location sympagic
7-1-2017	vMF1, vMF4, vMF9	
3-3-2017	MS	MS
8-3-2017		MS
13-3-2017	vMF3	
14-3-2017	vMF5, vMF9	
6-4-2017	MS	
7-4-2017	MS	MS
8-4-2017		vMF1
23-4-2017	MS	MS
26-4-2017	vMF2	vMF2
28-4-2017		IM
28-4-2017		IS
28-4-2017	vMF9	
29-4-2017		MS
29-4-2017	vMF5	
30-4-2017	vMF1	vMF1
30-4-2017		vMF2
2-5-2017	MS	MS
13-6-2017	vMF4	
14-6-2017	vMF9	

Sample processing

Samples for Chla determination were filtered onto GF/F filters (Whatman, Maidstone, UK). Filters were shock frozen in liquid nitrogen and stored at -80 °C until further analysis. Upon analysis Chla-filters were extracted in methanol overnight at 4 °C and the extract was analysed on a AE10 fluorometer (Turner Designs, San Jose, USA).

POC/N samples were filtered onto pre-combusted (8 hours, 450°C) GF/F filters and stored at -20 °C in precombusted (12 hours, 500°C) glass petridishes. Prior to analysis, samples were acidified (0.2ml of 0.2M HCl) and dried for 24 hours. The samples were subsequently packed into tin capsules. Most samples were analysed on a Euro EA 3000 elemental analyser (Hekatech, Wegberg, Germany). Approximately one quarter of the samples were analysed on a Flash EA 1112 elemental analyzer (Thermo Scientific, Milan, Italy) coupled to a Delta V Advantage IRMS (Thermo Scientific, Bremen, Germany), since stable isotope ratios needed to be determined for them in addition (for use in another part of the project). For intercalibration of the different elemental analysers, an acetanilide standard was used.

POP samples were filtered onto pre-combusted 0.7 µm GF/F filters and stored at -20 °C in

acid washed (10% HCl, 48 hours) scintillation vials. Upon analysis, the samples were digested with peroxodisulfate and analysed on a SAN+ autoanalyser (Skalar, Breda, Netherlands).

Nutrient samples were filtered using an acid washed syringe (10% HCl, 48 hours) and GF/F filters. Samples were stored at -20 °C in 15ml acid washed Falcon tubes. After thawing, the samples were run on a QuaAAtro autoanalyser (Seal Analytical, Mequon, U.S.A).

The bulk salinity was measured using a Symphony SP90M5 conductivity meter (VWR, Radnor, USA). Brine salinities were calculated from the in situ temperatures, using the experimental relationship (Cox, Weeks 1983):

$$S_{brine} = 1000/(1-54.11/T_{ice}) \quad [1])$$

where S_{brine} is the salinity in PSU and T_{ice} is the temperature of the ice in °C. Relative brine volume was calculated using the experimental relationship (Cox, Weeks 1983):

$$V_{brine} = S_{ice} * (0.0532 - \frac{4.919}{T_{ice}}) \quad [2])$$

where V_{brine} is the relative brine volume, S_{ice} is the bulk salinity in psu and T_{ice} is the temperature of the ice in °C.

Irradiance

To assess the sympagic light climate, downwelling photosynthetic active radiation (PAR) in air and at the ice-water interface was measured simultaneously using two cosine-corrected 2π PAR sensors coupled to a data logger (LI-1400). For the measurements at the ice-water interface, a hole in the ice was made through which a hinging arm was put in order to measure away from the hole. Measurements were taken underneath an undisturbed patch of snow located to the south of the hole in order to minimize the shading effect of the equipment and observer. Measurements were repeated after measuring the snow depth and the subsequent removal of approximately $5m^2$ of snow around the measuring point, in order to measure the light attenuation of the ice only.

Similar measurements using the two cosine-corrected 2π PAR sensors and data logger were performed at different depths for assessment of the pelagic light climate, both under the ice as in open water. Pelagic measurements under ice were performed through the same hole as the sympagic measurements. The pelagic light measurements in open water were done from a small tender away from the larger main vessel, to reduce the shading effect of the vessel used.
To correct for variability in the weather during sampling days, the relative transmittance was calculated for each site, and multiplied by the maximum value of incoming PAR on a clear day.

Physical data on sea ice and water column characteristics

Additional data on the ice cores was gathered and consisted of ice thickness, freeboard and snow depth. Each pelagic sampling was accompanied by a CTD cast (SD208, SAIV A/S, Norway), measuring vertical profiles of temperature, salinity and in situ fluorescence.

Statistical analysis

The relation between NO_3, PO_4, light and the stoichiometric ratios of carbon, nitrogen and phosphorus were assessed by means of linear mixed modelling, with replicates as a random effect, using the base package of R (version 3.4.2). Because the stoichiometric data were right skewed, the

stoichiometric ratios were log transformed before modelling. Significance was tested by means of one-way ANOVA.

Results

Nutrients and stoichiometric ratios of pelagic POM

The sampling was performed at three standard sampling stations; an inner basin (vMF1), an outer basin (vMF5) and a station just outside van Mijenfjorden (vMF9). In June, vMF1 could not be reached due to ice conditions.

Molar C:N ratios of pelagic POM (particulate organic matter) at the pelagic stations vMF1, vMF5 and vMF9 were relatively uniform across all depths (Figure 2), except from June, where C:N ratios at 5 and 15 m were higher than those sampled from greater depths ($p<0.01$).
The mean January C:N ratios were 10.1 ± 0.3 SD, 9.8 ± 0.5 SD and 9.2 ± 0.7 SD at vMF1, vMF5 and vMF9 respectively. March showed higher depth averaged C:N ratios with 13.8 ± 1.0 SD, 12.2 ± 1.5 SD and 10.7 ± 08 SD at vMF1, vMF5 and vMF9 respectively. The April means were considerably lower than in March, with 7.5 ± 1.7 SD, 6.5 ± 0.4 SD and 6.7 ± 0.2 SD at vMF1, vMF5 and vMF9. In June the mean C:N ratios at vMF5 and vMF9 were 7.7 ± 1.7 SD, and 7.4 ± 0.6 SD.

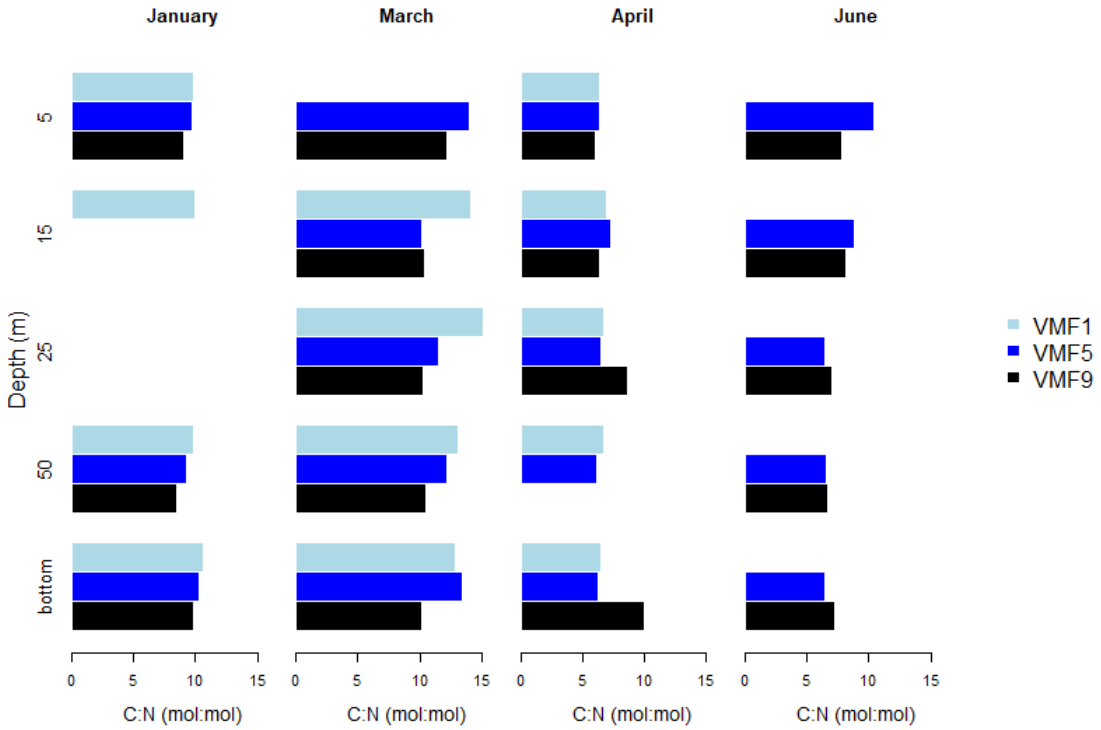

Figure 2. Molar C:N ratios at 5, 15, 25, 50 m water depth and close to the bottom, at vMF1, vMF5 and vMF9 in January, March, April and June.

In January and March the pelagic nitrate concentrations were fairly uniform across all depths (Table 2). Nitrate concentrations in April and June still showed a high degree of similarity, but deeper layers tended to have higher nitrate concentrations compared to layers closer to the surface.
Mean nitrate concentrations in January were 8.93 ± 0.20 SD, 8.79 ± 0.10 SD and 10.60 ± 1.67 SD µmol/l at vMF1, vMF5 and vMF9 respectively, and increased into March with means of 10.20 ± 0.35 SD, 10.51 ± 0.16 SD and 11.04 ± 0.82 SD µmol/l at vMF1, vMF5 and vMF9 respectively. Nitrate

concentrations dropped considerably towards April, with a mean of 6.31 ± 4.31 SD, 4.68 ± 2.24 SD and 4.23 ± 0.94 SD µmol/l in April at vMF1, vMF5 and vMF9. In April, the surface layer (5m) at vMF1 was almost depleted of nitrate (0.23 µmol/l), while the layer at 25 m and close to the bottom were still at concentrations comparable to January/March concentrations. Nitrate concentrations dropped further in June, towards an mean of 2.06 ± 1.17 SD µmol/l at vMF5 and a mean of 3.12 ± 4.27 SD µmol/l at vMF9.

Table 2. Nitrate concentrations (µmol/l) at depths: 5, 15, 25, 50, bottom for vMF1, vMF5 and vMF9 in January, March, April and June.

NO_3	January			March			April			June		
(µmol/l)	vMF 1	vMF 5	vMF 9	vMF 1	vMF 5	vMF 9	vMF 1	vMF 5	vMF 9	vMF 1	vMF 5	vMF 9
5	9.00	8.88	9.39	10.24	10.53	11.20	0.23	3.04	3.17	n/a	1.15	0.02
15	9.00	8.74	9.75	9.97	10.72	9.64	6.59	2.35	3.26	n/a	1.29	0.12
25	n/a	n/a	n/a	10.09	10.32	11.82	10.12	4.42	5.14	n/a	1.85	0.89
50	8.64	8.86	10.20	9.93	10.37	11.27	n/a	5.55	4.63	n/a	1.93	4.57
bottom	9.08	8.66	13.07	10.79	10.60	11.26	8.34	8.02	4.93	n/a	4.07	10.00

Molar C:P ratios peaked in March and showed high variation across different depths, with 169 ± 38 for vMF1, 160 ± 45 SD for vMF5 and 203 ± 20 SD for vMF9 (Figure 3). The C:P ratios were on average lowest in April, with 144 ± 51 SD, 106 ± 17 SD and 119 ± 14 SD for vMF1, vMF5 and vMF9 respectively. June averages had increased compared to April to 145 ± 38 SD for vMF5 and 133 ± 27 for vMF9.

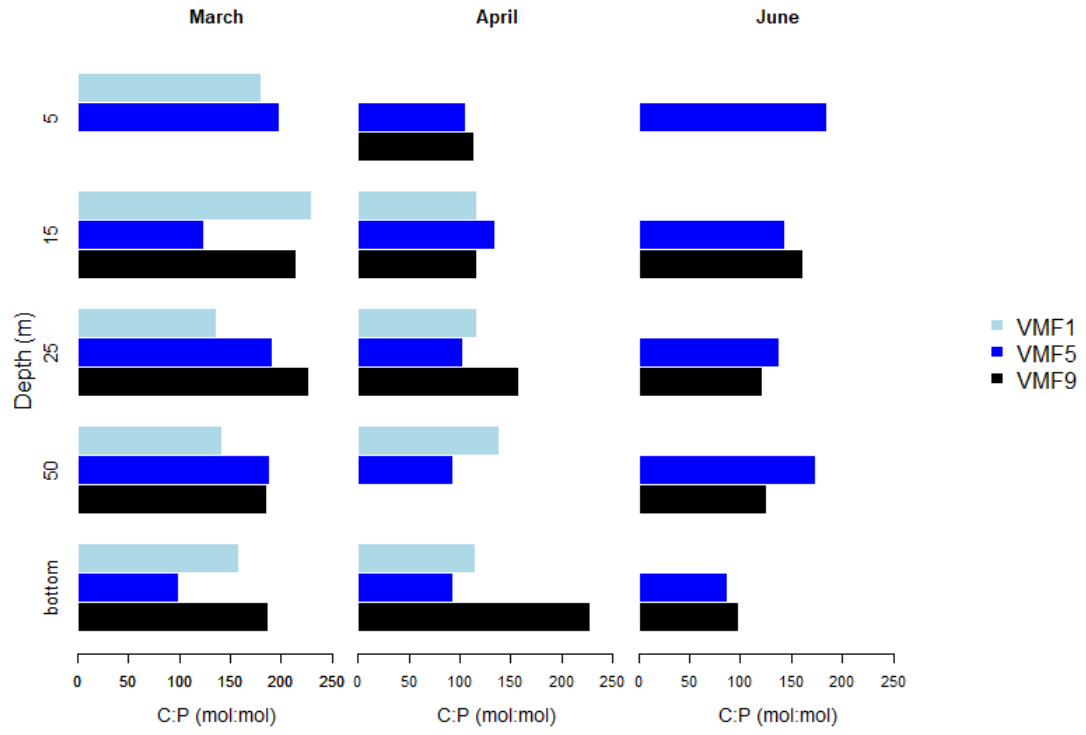

Figure 3. Molar C:P ratios at 5, 15, 25, 50 m water depth and at the bottom, at vMF1, vMF5 and vMF9 in March, April and June.

Phosphate concentrations were generally low (<0.8 µmol/l), but showed similar trends as the nitrate concentrations. January phosphate concentrations averaged 0.53 µmol/l and by March they had slightly increased to an average of 0.63 µmol/l. Phosphate concentrations dropped towards an average of 0.34 µmol/l in April, and a further drop towards an average of 0.28 µmol/l was measured in June (Table 3).

Table 3. Phosphate concentrations (µmol/l) at depths: 5, 15, 25, 50, bottom for vMF1, vMF5 and vMF9 in March, April and June.

PO_4	January			March			April			June		
(µmol/l)	vMF 1	vMF 5	vMF 9	vMF 1	vMF 5	vMF 9	vMF 1	vMF 5	vMF 9	vMF 1	vMF 5	vMF 9
5	0.48	0.48	0.54	0.61	0.47	0.69	0.08	0.24	0.23	n/a	0.19	0.04
15	0.46	0.48	0.56	0.63	0.58	0.64	0.42	0.19	0.24	n/a	0.20	0.12
25	n/a	n/a	n/a	0.59	0.61	0.75	0.61	0.31	0.38	n/a	0.22	0.20
50	0.48	0.48	0.63	0.59	0.62	0.70	n/a	0.38	0.35	n/a	0.23	0.47
bottom	0.50	0.45	0.82	0.61	0.64	0.70	0.48	0.52	0.36	n/a	0.38	0.78

Pelagic chlorophyll a and POC

Chlorophyll a concentrations (Table 4) were uniform throughout the water column in January and March. January chlorophyll a concentrations were 0.03, 0.04 and 0.05 µg/l at vMF1, vMF5 and vMF9 respectively. By March the chlorophyll a concentrations had increased a little towards 0.7, 0.7, and 0.6 µg/l at vMF1, vMF5 and vMF9, but were still considered low.

High levels of chlorophyll a were measured in April at all stations, with the highest level in the uppermost layer, gradually decreasing downwards. Chlorophyll a concentrations at vMF1 decreased from 15.16 µg/l at 5m, to 6.28 µg/l at 15m, to 1.82 µg/l at 25 m and to 0.46 µg/l close to the bottom. At vMF5 chlorophyll a concentrations were 15.46, 13.42, 12.09 and 6.85 µg/l at 5m, 25m, 50m and close to the bottom, respectively. Chlorophyll a concentrations in April at vMF9 were 13.79, 11.04, 10.76, 8.51 and 5.20 µg/l at 5m, 15m, 25m, 50m and near the bottom.

Chlorophyll a concentrations in June at vMF5 were 0.47, 0.60, 0.60 and 0.40 µg/l at 5m, 15m, 25m and 50m, respectively. Most chlorophyll a was found close to the bottom, with a concentration of 1.03 µg/l. Chlorophyll a concentrations from vMF9 measured 3.31, 0.97, 4.67, 2.75 and 0.95 µg/l at 5m, 15m, 25m, 50m and near the bottom respectively.

Table 4. Seasonal development of chlorophyll a concentrations between January and June, at stations vMF1, vMF5 and vMF9.

Chl a	January			March			April			June		
(µg/l)	vMF 1	vMF 5	vMF 9	vMF 1	vMF 5	vMF 9	vMF 1	vMF 5	vMF 9	vMF 1	vMF 5	vMF 9
5	0.03	0.04	0.05	0.07	0.07	0.06	15.16	15.46	13.79	n/a	0.47	3.31
15	0.03	0.04	0.05	0.07	0.07	0.06	6.28	n/a	11.04	n/a	0.60	0.97
25	n/a	n/a	n/a	0.07	0.07	0.06	1.82	13.42	10.76	n/a	0.60	4.67
50	0.03	0.04	0.06	0.07	0.07	0.06	n/a	12.09	8.51	n/a	0.40	2.75
bottom	0.03	0.04	0.05	0.08	0.09	0.07	0.46	6.85	5.20	n/a	1.03	0.95

The ratio of POC:Chl a (weight:weight) was calculated to assess the contribution of algae to the total seston pool filtered (Table 5). The POC:Chl ratio was highest in January, with values ranging between 1140 and 2212 at vMF1, between 1623 and 1848 at vMF5 and between 1298 and 2417 at vMF9. March POC:Chl ratios were significantly lower at all stations ($p<0.01$), with values between 1054 and 1635 at vMF1, between 884 and 1386 at vMF5 and between 588 and 1100 at vMF9.

The April sampling showed a dramatic drop in POC:Chl ratios ($p<0.0001$). At vMF1 POC:Chl ratios ranged from 30 to 53 in the upper 25 meters of the water column, close to the bottom the POC:Chl ratio was 210. POC:Chl ratios at vMF5 were uniform throughout the water column, values were between 25 and 29. VMF9 results were similar to the results from vMF5, POC:Chl ratios were between 27 and 34.

In June POC:Chl ratios had increased compared to April ($p<0.01$). June value ranged from 196 to 811 at vMF5 and from 61 to 281 at vMF9.

Table 5. Seasonal development of the ratio of POC:Chl (weight:weight).

	January			March			April			June		
POC:Chl a	vMF 1	vMF 5	vMF 9	vMF 1	vMF 5	vMF 9	vMF 1	vMF 5	vMF 9	vMF 1	vMF 5	vMF 9
5	2212	1848	2417	1313	1386	1100	30	27	29	n/a	760	162
15	1813	n/a	n/a	1405	884	629	33	n/a	32	n/a	541	281
25	n/a	n/a	n/a	1146	1206	610	53	29	27	n/a	461	61
50	2553	1623	2075	1054	1356	709	n/a	25	31	n/a	811	107
bottom	1440	1635	1298	1635	1102	588	210	29	34	n/a	196	116

CTD results

Chlorophyll fluorescence measurements from the CTD casts (for graphs, view Appendix B) taken in March were uniform across all depths and showed close to zero chlorophyll fluorescence for vMF1 and vMF5 and were between 0.1 and 0.2 µg/l at vMF9. The salinity at the different stations was also fairly constant across depths, with salinities of 34.65 psu at vMF1, 35.70 at vMF5 and 35.15 psu at vMF9, all ± 0.05 psu (range). The temperature at vMF1 showed a gradual incline from -1.4 °C at the surface to -1.1 °C at the bottom. At vMF5 the temperature in the upper 20 meters of the water column ranged between -1.4 °C and -1.2 °C. At 20 meters the temperature increased sharply to -0.8 °C and gradually increased towards -0.5 °C at 90 meters of water depth. The water was warmer outside of the fjord basin, than inside of the basin. The water temperature at vMF9 was 1.6 °C at the surface and gradually dropped to 1.4 °C at the bottom.

In April the CTD casts registered clear signs of increased primary production at all stations. At vMF1, chlorophyll fluorescence was elevated in the upper 25 meters were values were around 0.5 and 1.7 µg/l, with a peak fluorescence at one meter water depth of 4.0 µg/l. At vMF5 and vMF9 chlorophyll fluorescence was elevated throughout the water column. At vMF5 values were between 1.6 and 3.1 µg/l in the upper 55 meters of the water column, after which they gradually declined to values between 0.1 and 0.5 µg/l close to the bottom. Fluorescence values at vMF9 were between 1.8 and 4.0 µg/l in the upper 55 meters and showed a gradually declining trend towards values between 0.3 and 1.2 µg/l close to the bottom. The salinity at vMF1 was fairly uniform throughout the water column with a gradual increase from 34.7 to 34.9 psu, except for a one meter thick layer at the surface, which had a salinity of 32.5 psu. The salinity at vMF5 was 34.6 psu at the surface, gradually increased to 34.8 psu at 35 meters and showed a further slight increase to 34.9 psu near the bottom. The salinity at vMF9 increased from 34.4 psu at the surface to 34.6 psu at the bottom. The water temperature at vMF1 was around -1.6 °C with minor excursions towards -1.4 and -1.7 °C in the upper 25 meters. At vMF5, the water temperature decreased slightly from -1.4 °C at the surface, to -1.6 °C near the bottom. At vMF9, the water temperature at the surface was -1.0 °C, decreased slightly to -1.1 °C at 45 meters, where the temperature increased back to -1.0 °C and continued to increase to -0.8 at 115 meters, and finally showed a sharper increase in the last 10 meters near the bottom to -0.5°C.

The chlorophyll fluorescence data from the first 30 meters from the June cast at vMF5 were missing. Fluorescence in the rest of the water column was fairly homogenous, with values ranging between 0.3 and 1.5 µg/l. At vMF9 there was a distinct deep chlorophyll maximum between 30 and 100 meters of water depth. with a values between 1.5 and 11.9 µg/l. The salinity at vMF5 in the upper 3 meters was 33.0 psu, sharply increased to 34.5 psu at 8 meters and gradually increased further to 34.6 psu near the bottom. At vMF9 the salinity increased from 34.3 psu at the surface towards 35.0 near the bottom. At vMF5 matched the sharp increase in salinity in the upper layer was mirrored by a sharp decrease in temperature. In the upper layer, the temperature dropped from 2.9

°C at the surface to 0.7 °C at 8 meters of water depth. From the 8 meter mark, the temperature decrease further to -1.3 °C close to the bottom. At vMF9, the temperature profile mirrored the fluorescence profile in a way that the lowest temperatures coincided with the highest fluorescence. The surface temperature was 3.9 °C, decreased sharply to 2.4 °C at 8 meters of water depth and further decreased to 1.4 °C at a water depth of 25 meters. From 25 to 60 meters of water depth, the temperature was between 1.2 and 1.4 °C and increased to 2.7 °C at the 100 meter depth mark after which it decrease again to 2.2 °C near the bottom.

Modelling results

Using a linear model for the dependence of C:N on nitrate concentrations a positive relationship was found for the set containing all samples from April, May and June ($p<0.00001$) (Figure 4, left panel). C:N ratios showed no dependence on the peak PAR levels ($p>0.8$) (Figure 4, right panel).

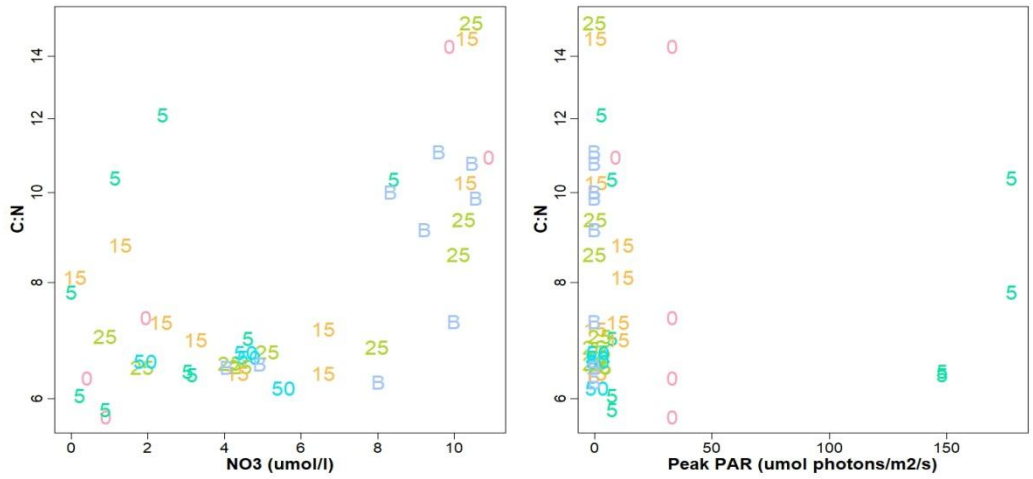

Figure 4. Scatterplots showing the C:N ratio versus nitrate (left panel) and light (right panel) for the pelagic samples from April and onward. The numbers denote the depth at which the samples were taken, with B standing for "bottom".

C:P ratios versus phosphate concentrations did not show a linear trend with phosphate concentrations ($p>0.1$) or light ($p>0.7$) (Figure 5).

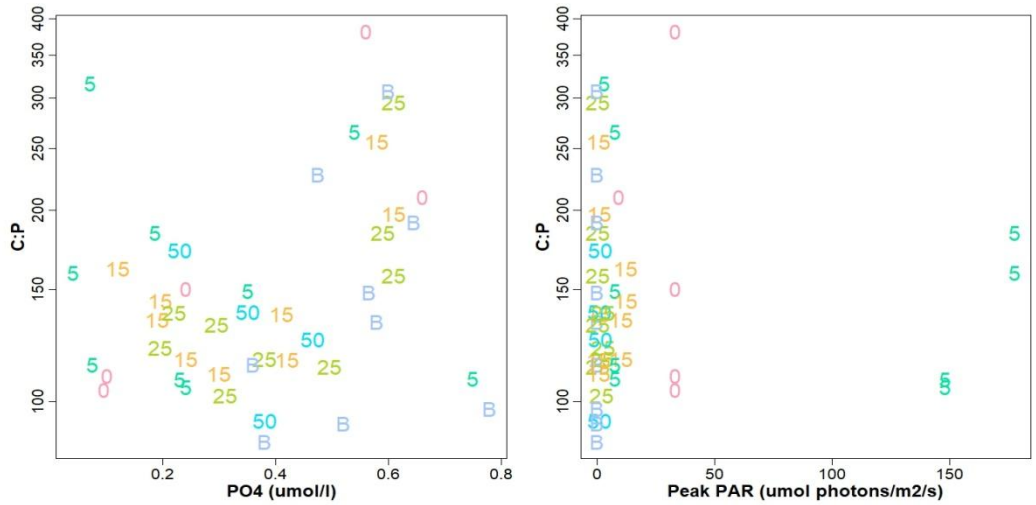

Figure 5. Scatterplots showing the C:P ratio versus phosphate (left panel) and light (right panel) for the pelagic samples from April and onward. The numbers denote the depth at which the samples were taken, with B standing for "bottom".

Changes in N:P ratios did not correlate with changes in either nitrate ($p>0.1$), phosphate ($p<0.1$) or light ($p>0.7$) (Figure 6).

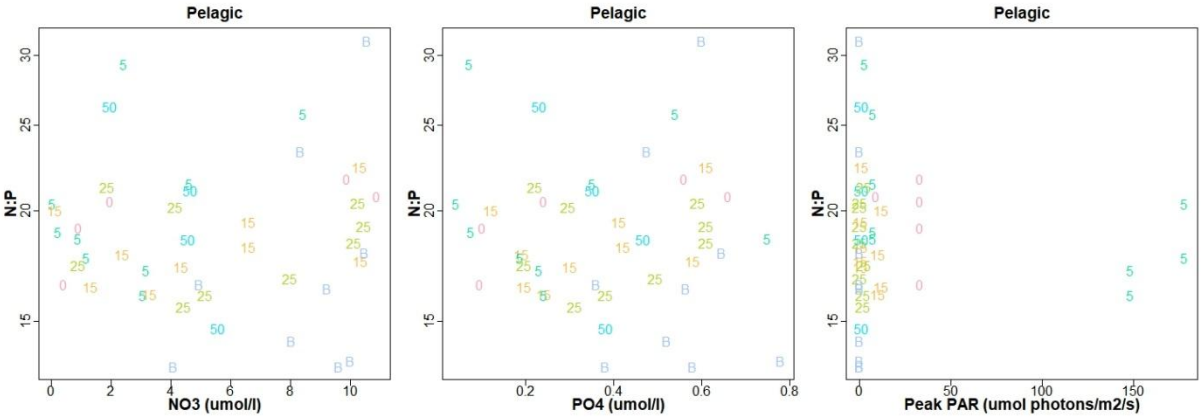

Figure 6. Scatterplots showing the N:P ratio versus nitrate (left panel), phosphate (middle panel) and light (right panel) for the pelagic samples from April and onward. The numbers denote the depth at which the samples were taken, with B standing for "bottom".

Nutrients and stoichiometric ratios of sympagic POM

Sea ice algae were sampled along a transect in the inner part of the fjord, consisting of a main station (MS) where a number of autonomous instruments were deployed in early March, the two innermost stations of the FAABulous pelagic transect, vMF1 and vMF2, and two more stations closer to the shore in shallower waters, IS and IM. The exact coordinates of these stations can be found in Appendix A.

Temporal patterns in nutrients and sea ice algal stoichiometry (at MS)

Sea ice algal assemblages were studied at the main station from early March until early May. The C:N ratios at the main sampling station were highest in March (Figure 7) for both the 0-3 cm

section (panel a) as well as the 3-10 cm section (panel b). Apart from this, the C:N ratios for the 0-3 cm and 3-10 cm section lacked a clear trend.

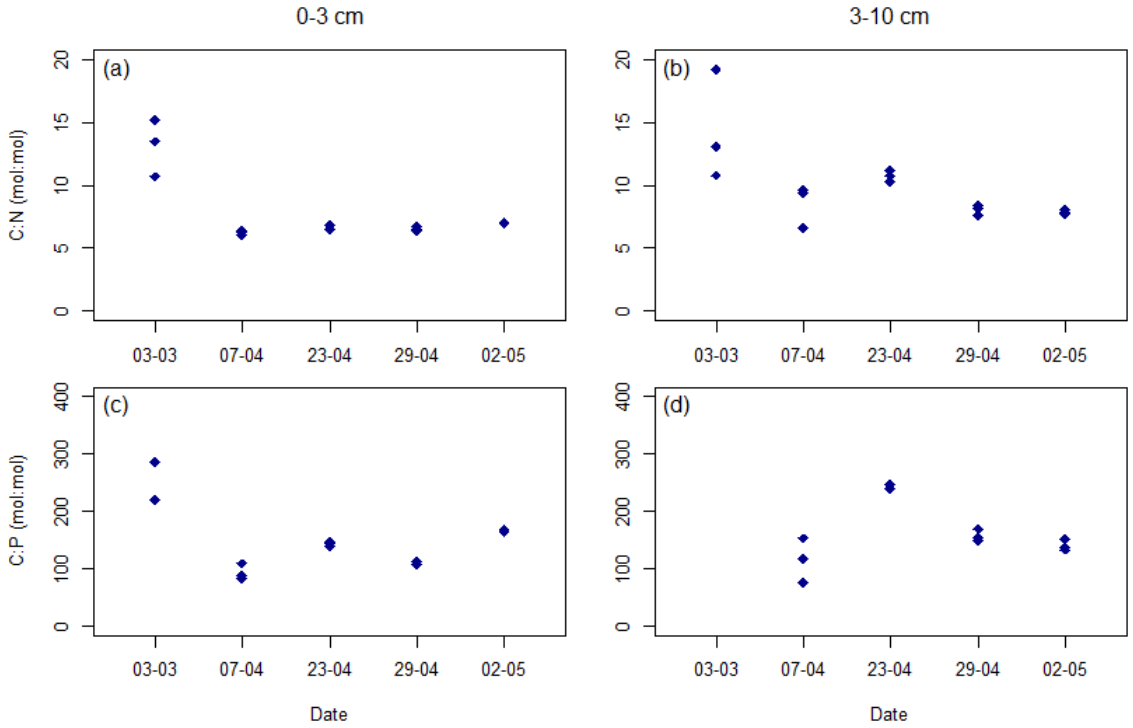

Figure 7. Seasonal development of molar C:N and C:P ratios at station MS. Panel a, C:N ratio 0-3 cm; panel b, C:N ratio 3-10 cm; panel c, C:P ratio 0-3 cm; panel d, C:P ratio 3-10 cm.

Nitrate and phosphate concentrations did not show a clear trend in the time series. Nutrient concentrations were generally lower in the 3-10 cm section, compared to the 0-3 section (Table 6). Mean nitrate concentrations in the 0-3 cm section were 4.61, 4.05, 14.51, 4.36 and 0.69 µmol/l on the 3rd of March, the 7th, 23rd and 29th of April and the 2nd of May respectively. The matching phosphate concentrations for the same dates and core section were: 0.66, 0.45, 0.96, 0.57 and 1.46 µmol/l. Mean nitrate concentrations in the 3-10 cm section were 1.70, 0.43, 1.17, 0.28 and 0.21 µmol/l on the 3rd of March, the 7th, 23rd and 29th of April and the 2nd of May respectively. The matching phosphate concentrations for the same dates and core section were: 0.35, 0.06, 0.08, 1.03 and 0.12 µmol/l.

Table 6. Nitrate and phosphate concentrations (µmol/l) at station MS taken between the 3rd of March to the 2nd of May. Values represent the arithmetic mean of three pools each.

	3/3		7/4		23/4		29/4		2/5	
(µmol/l)	NO_3	PO_4	NO_3	PO_4	NO_3	PO_4	NO_3	PO_4	NO_3	PO_4
0-3 cm	4.61	0.66	4.05	0.45	14.51	0.96	4.36	0.57	0.69	1.46
SD	*± 2.58*	*± 0.54*	*± 0.73*	*± 0.11*	*± 2.84*	*± 0.06*	*± 0.71*	*± 0.56*	*± 0.17*	*± 0.33*
3-10 cm	1.70	0.35	0.43	0.06	1.17	0.08	0.28	1.03	0.21	0.12
SD	*± 0.09*	*± 0.36*	*± 0.25*	*± 0.02*	*± 0.68*	*± 0.02*	*± 0.05*	*± 0.82*	*± 0.17*	*± 0.01*

Chlorophyll a concentrations at station MS in the 0-3 cm section were low on the 3rd of March (mean = 0.02 mg/m^2, Table 7). By the 7th of April this had increased significantly ($p<0.001$) to a mean concentration of 4.52 mg/m^2. Another significant increase ($p<0.01$) was measured on the 23th of April, with a mean chlorophyll concentration of 20.86 mg/m^2. By the 29th of April the mean

concentration had dropped ($p<0.01$) to 12.59 mg/m^2, but did not drop further towards the 2nd of May (mean = 13.82 mg/m^2)

Chlorophyll a concentrations on the 3rd of March in the 3-10 cm section were not different ($p=0.4$) from those of the 0-3 cm section. In April and May, the 3-10 cm sections showed consistently lower chlorophyll a concentrations than the 0-3 cm sections ($p<0.001$). Comparing the different samples from the 3-10 cm sections, chlorophyll a concentrations were higher ($p<0.05$) on the 7th of April (mean = 1.43 mg/m^2), compared to the March concentrations (mean = 0.08 mg/m^2) . On the 23rd of April chlorophyll a concentrations were again higher ($p<0.05$, mean = 4.17 mg/m^2) than the previous sampling moment. On the 29th chlorophyll a concentrations were lower ($p<0.05$, mean = 2.53 mg/m^2) than on the 23rd of April, but increased again ($p<0.05$) towards the 2nd of May (mean = 4.17 mg/m^2).

POC:Chl a ratios in the 0-3 cm sections were significantly higher (mean = 1338, $p<0.001$) at the start of the sampling period in March compared to later in the season. Throughout April, the ratios remained similar (37, 26 and 32 at the 7th, 23rd and 29th of April, respectively), but increased again in May (mean = 55, $p<0.01$). Similar to the 0-3 cm sections, the POC:Chl a ratios in the 3-10 cm sections in March were an order of magnitude higher than later in the season. POC:Chl a ratios at the 7th, 23rd and 29th of April and the 2nd of May were 72, 37, 54 and 32, respectively.

Table 7. Chlorophyll a concentrations (mg/m^2) and POC:Chl a ratios at station MS from early March until early May. Values represent the arithmetic mean of three pools each.

	3/3		7/4		23/4		29/4		2/5	
	0-3 cm	3-10 cm	0-3 cm	3-10 cm	0-3 cm	3-10 cm	0-3 cm	3-10 cm	0-3 cm	3-10 cm
Chl a (mg/m2)	0.02	0.08	4.52	1.43	20.86	4.17	12.59	2.53	13.82	4.17
SD	*± 0.00*	*± 0.02*	*± 0.81*	*± 0.66*	*± 0.82*	*± 0.63*	*± 0.98*	*± 0.41*	*± 0.69*	*± 0.73*
POC:Chl a	1338	872	37	72	26	37	32	54	55	32
SD	*± 237*	*± 293*	*± 9*	*± 29*	*± 3*	*± 4*	*± 3*	*± 6*	*± 10*	*± 3*

Spatial variability: a) Transect along the fjord axis

The C:N ratios for the transect stations IS, IM and MS were not different from each other ($p=0.46$) with means of 6.2, 6.5 and 6.5 respectively (Figure 8). C:N ratios for vMF1(mean = 7.7) and vMF2 (mean = 10.5) were higher than the other stations ($p<0.001$). The C:P ratios showed the same trend as the C:N ratios, no difference ($p=0.34$) between IS (mean = 119), IM (mean = 120) and MS (mean = 109), but higher C:P ratios at vMF1 (mean = 207) and vMF2 (mean = 248) ($p<0.001$).

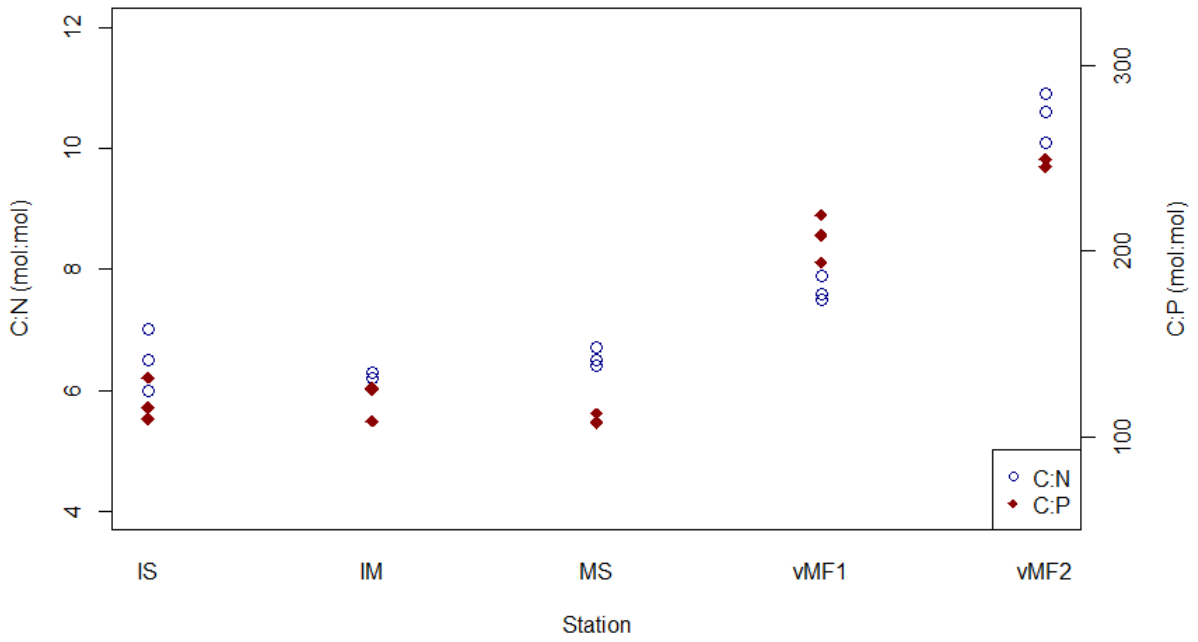

Figure 8. Molar C:N and C:P ratios in the lower 0-3 cm section of the ice cores taken from the transect.

The nitrate concentrations in the 0-3 cm section showed a consistent decline from station IS towards vMF2, with 16.21, 5.36, 4.36, 0.71, and 0.21 µmol/l for IS, IM, MS, vMF1 and vMF2 respectively (Table 8). Phosphate concentrations lacked a trend and ranged between 0.27 µmol/l at vMF2 and 1.81 µmol/l at vMF1. Nutrient concentration in the 3-10 cm section were generally low and lacked a clear trend with nitrate ranging between 0.08 and 1.08 µmol/l and phosphate between 0.01 and 1.03 µmol/l.

Table 8. Nitrate and phosphate concentrations (µmol/l) along the transect. Values represent the arithmetic mean of three pools each.

	IS		IM		MS		vMF1		vMF2	
(µmol/l)	NO_3	PO_4	NO_3	PO_4	NO_3	PO_4	NO_3	PO_4	NO_3	PO_4
0-3 cm	16.21	0.46	5.36	1.16	4.36	0.57	0.71	1.81	0.21	0.27
SD	*± 2.53*	*± 0.26*	*± 0.56*	*± 0.18*	*± 0.71*	*± 0.56*	*± 0.21*	*± 0.67*	*± 0.03*	*± 0.06*
3-10 cm	0.56	0.21	1.08	0.23	0.28	1.03	0.09	1.06	0.08	0.01
SD	*± 0.43*	*± 0.07*	*± 0.24*	*± 0.13*	*± 0.05*	*± 0.82*	*± 0.06*	*± 0.89*	*± 0.01*	*± 0.01*

Chlorophyll a concentrations along the transect in the 0-3 cm section were similar from station IS through to vMF1, with mean concentrations of 15.52, 12.20, 12.59 and 14.23 mg/m^2 at stations IS, IM, MS and vMF1 respectively, but were significantly lower at vMF2 with a mean value of 3.63 mg/m^2 ($p<0.001$)(Table 9). In the 3-10 cm sections, the chlorophyll a concentrations fluctuated without a showing a trend. The mean concentrations were on the lowest at vMF2 and IM, with vaues of 0.55 and 0.89 mg/m^2, respectively. Higher concentrations were measured at IS and MS (1.57 and 2.53 mg/m^2) and the highest at vMF1 (mean = 3.96 mg/m^2).

The POC:Chl a ratios in the 0-3 cm section were similar along the transect (77, 48, 57 and 73 mg/m^2 at IS, IM, vMF1 and VMF2), except at station MS, which had a lower ratio of 32 ($p<0.01$). In the 3-10 cm section, POC:Chl a ratios were similar at stations IS and IM (124 and 105), were lower

further along the transect at station MS and vMF1 (54 and 42, $p<0.01$) and were higher again at vMF2 (243, $p<0.01$).

Table 9. Chlorophyll a concentrations (mg/m^2) and POC:Chl a ratios along the transect. Values represent the arithmetic mean of three pools each.

	IS		IM		MS		vMF1		vMF2	
	0-3 cm	3-10 cm	0-3 cm	3-10 cm	0-3 cm	3-10 cm	0-3 cm	3-10 cm	0-3 cm	3-10 cm
Chl a (mg/m2)	15.52	1.57	12.20	0.89	12.59	2.53	14.23	3.96	3.63	0.55
SD	*± 1.88*	*± 0.26*	*± 0.49*	*± 0.04*	*± 0.98*	*± 0.41*	*± 0.19*	*± 0.26*	*± 1.63*	*± 0.29*
POC:Chl a	77	124	48	105	32	54	57	42	73	243
SD	*± 24*	*± 14*	*± 7*	*± 16*	*± 3*	*± 6*	*± 9*	*± 1*	*± 8*	*± 87*

Spatial variability: b) Low snow versus high snow

Snow depths at the sampling sites were categorized to be 'low' within the range of 0-4 cm, and as 'high' for snow depths between 20 and 27 cm.

The C:N ratios in the 0-3 cm section did not differ ($p = 0.09$) on the 23rd of April (Figure 9, panel a). Over the course of the ten day sampling period, C:N ratios from sea ice POM collected underneath high snow areas showed no significant change ($p = 0.23$), with mean values of 6.7,6.5 and 7.0 on the 23rd and 26th of April and the 2nd of May respectively. C:N ratios from the low snow areas however, increased significantly from 7.5 to 11.6 to 12.7 ($p < 0.01$).

Overall, C:P ratios were consistently higher under low snow conditions, compared to high snow conditions ($p < 0.01$), at all three sampling moments. Mean C:P ratios from 0-3 cm under high snow were lower ($p < 0.01$) on the 23rd of April compared to the 26th of April and the 2nd of May, 144 versus 177 and 166 respectively. C:P ratios increased in the 0-3 cm sections that were sampled beneath low snow areas (Figure 9, panel c) from a mean of 204 on the 23rd of May to 285 and 298 on the 26th of April and the 2nd of May respectively.

The C:N and C:P ratios in the 3-10 cm sections from the low snow areas did not change during the sampling period (Figure 9 panels b, d). The mean C:N ratio for the entire period was 10.4 ± 1.4 SD, and the mean C:P ratio was 203 ± 46 SD. The mean C:N ratio for 3-10 cm, high snow, was lower at station MS on the 2nd of May ($p < 0.001$) compared to the two previous sampling days, with a mean of 7.8 ± 0.2 SD on the 2nd of May, compared to means of 10.8 ± 0.5 SD and 10.3 ± 0.6 SD on the 23rd and 26th of April. C:P ratios at station MS on the 23rd of April, under high snow, were higher than on the two following sampling days ($p < 0.01$), with means of 242 ± 4, 178 ± 18 and 141 ± 9 on the 23rd and 26th of April and the 2nd of May, respectively.

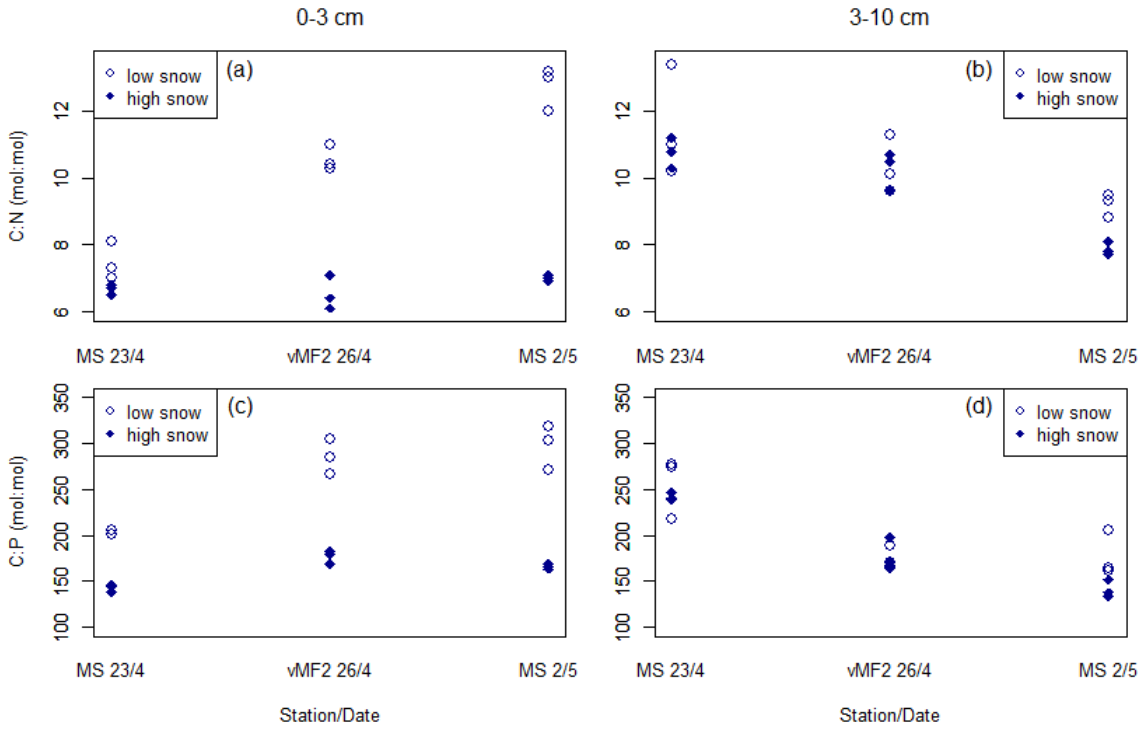

Figure 9. Differences in sea ice POM stroichiometric ratios between sampling locations with low snow and high snow: Molar C:N ratios for the 0-3 cm sections (a), C:N ratios the 3-10 cm sections (b), C:P ratios for the 0-3 cm sections (c) and C:P ratios for the 3-10 cm sections (d).

Over the course of the 10 day sampling period nitrate concentrations declined rapidly in both core sections, taken from both low and high snow areas (Table 9). Nitrate concentrations from the low snow areas declined from 3.11 to 0.17 µmol/l and 0.31 to 0.00 µmol/l for the 0-3 cm and 3-10 cm sections respectively. Nitrate concentrations taken from underneath the high snow cover, declined from 14.51 to 0.69 µmol/l and 1.17 to 0.21 µmol/l for the 0-3 cm and 3-10 cm sections respectively. At the start of the sampling period, nitrate concentrations were however lower in low snow areas, compared to high snow areas and in the 0-3 cm sections, compared to the 3-10 cm sections. Phosphate concentrations didn't show a trend over time, but were lower in the 3-10 cm section.

Table 10. Nitrate and phosphate concentrations (µmol/l) from low and high snow sampling locations in the two lowermost sections of the ice cores. Values represent the arithmetic mean (±SD) of three pools each.

	MS 23/4		vMF2 26/4		MS 2/5	
0-3cm	NO_3 (µmol/l)	PO_4 (µmol/l)	NO_3 (µmol/l)	PO_4 (µmol/l)	NO_3 (µmol/l)	PO_4 (µmol/l)
Low snow	3.11 ± *1.81*	1.56 ± *0.33*	0.79 ± *0.10*	0.61 ± *0.27*	0.17 ± *0.05*	1.83 ± *0.16*
High snow	14.51 ± *2.84*	0.96 ± *0.06*	2.72 ± *0.22*	0.29 ± *0.07*	0.69 ± *0.17*	1.46 ± *0.33*

	MS 23/4		vMF2 26/4		MS 2/5	
3-10cm	NO_3 (µmol/l)	PO_4 (µmol/l)	NO_3 (µmol/l)	PO_4 (µmol/l)	NO_3 (µmol/l)	PO_4 (µmol/l)
Low snow	0.31 ± *0.17*	0.07 ± *0.02*	0.17 ± *0.11*	0.05 ± *0.01*	0.00 ± *0.01*	0.07 ± *0.02*
High snow	1.17 ± *0.68*	0.08 ± *0.02*	0.6 ± *0.01*	0.05 ± *0.01*	0.21 ± *0.17*	0.12 ± *0.01*

The mean chlorophyll a concentrations in the 0-3 cm sections did not differ on the 23rd of April between high and low snow (20.86 vs 23.36 mg/m^2)(Table 11). On the 26th of April, chlorophyll a concentrations were a little higher under low snow areas, with a mean of 6.20 mg/m^2, compared to a mean of 4.77 mg/m^2 under high snow ($p<0.05$). On the 2nd of May, higher chlorophyll a concentrations were found under high snow, compared to low snow (13.82 vs 8.95 mg/m^2, ($p<0.01$)).

Mean chlorophyll a concentrations in the 3-10 cm sections were consistently higher under high snow, compared to low snow cover (4.17 vs 1.37 mg/m^2, 1.10 vs 0.58 mg/m^2 and 4.17 vs 0.93 mg/m^2 at the 23rd and 26th of April and the 2nd of May, respectively, ($p<0.01$).

The mean POC:Chl a ratios in the 0-3 cm sections were consistently lower under high snow, compared to low snow areas (25 vs 38, 25 vs 66 and 55 vs 106 at the 23rd and 26th of April and the 2nd of May, respectively, ($p<0.01$). A similar trend was found in the 3-10 cm sections (37 vs 97, 65 vs 146 and 32 vs 148 at the 23rd and 26th of April and the 2nd of May, respectively, ($p<0.01$).

Table 11. Chlorophyll a concentrations (mg/m^2) and POC:Chl a ratios from low and high snow sampling locations in the two lowermost sections of the ice cores. Values represent the arithmetic mean (±SD) of three pools each.

	MS 23/4		vMF2 26/4		MS 2/5	
0-3cm	Chl a (mg/m2)	POC:Chl a	Chl a (mg/m2)	POC:Chl a	Chl a (mg/m2)	POC:Chl a
Low snow	23.36 *± 4.00*	38 *± 0*	6.20 *± 0.62*	66 *± 5*	8.95 *± 0.71*	106 *± 6*
High snow	20.86 *± 0.82*	25 *± 3*	4.77 *± 0.34*	25 *± 1*	13.82 *± 0.69*	55 *± 10*

	MS 23/4		vMF2 26/4		MS 2/5	
3-10cm	Chl a (mg/m2)	POC:Chl a	Chl a (mg/m2)	POC:Chl a	Chl a (mg/m2)	POC:Chl a
Low snow	1.37 *± 0.36*	97 *± 24*	0.58 *± 0.09*	146 *± 32*	0.93 *± 0.13*	148 *± 35*
High snow	4.17 *± 0.63*	37 *± 4*	1.10 *± 0.12*	65 *± 11*	4.17 *± 0.73*	32 *± 3*

Linear modelling results

A linear relationship was found between the log/log transformed data of nitrate concentration and C:N ratios for the 0-3 cm sections of the ice cores taken in April and May (Figure 10, left panel). March samples were excluded, since the POC:Chl a ratios suggested that a large fraction of the material sampled was not of autotrophic origin. The relationship found could be best approximated by the formula: $\ln(C:N) = 2.086 - 0.0858 \ln(NO3)$, $p<0.001$.

The log transformed C:N ratios in the 0-3 cm sections exhibited a linear relationship with the untransformed peak irradiance levels (Figure 10, right panel). The best linear fit for this relationship was: $C:N = \exp(1.8746 + 0.005974 * \text{Peak PAR})$, $p<0.0001$.

A similar relationship to the one between C:N and irradiance was found between the C:P ratios and irradiance, which was best approximated by: $C:P = \exp(4.8931 + 0.008714 * \text{Peak PAR})$, $p<0.001$ (Figure 11, right panel).

No linear relationship was found between C:P ratios and phosphate concentrations (Figure 11, left panel. Similarly, the N:P ratios failed to show a trend with nitrate and phosphate concentrations and irradiance (Figure 12, left, middle and right panel, respectively).

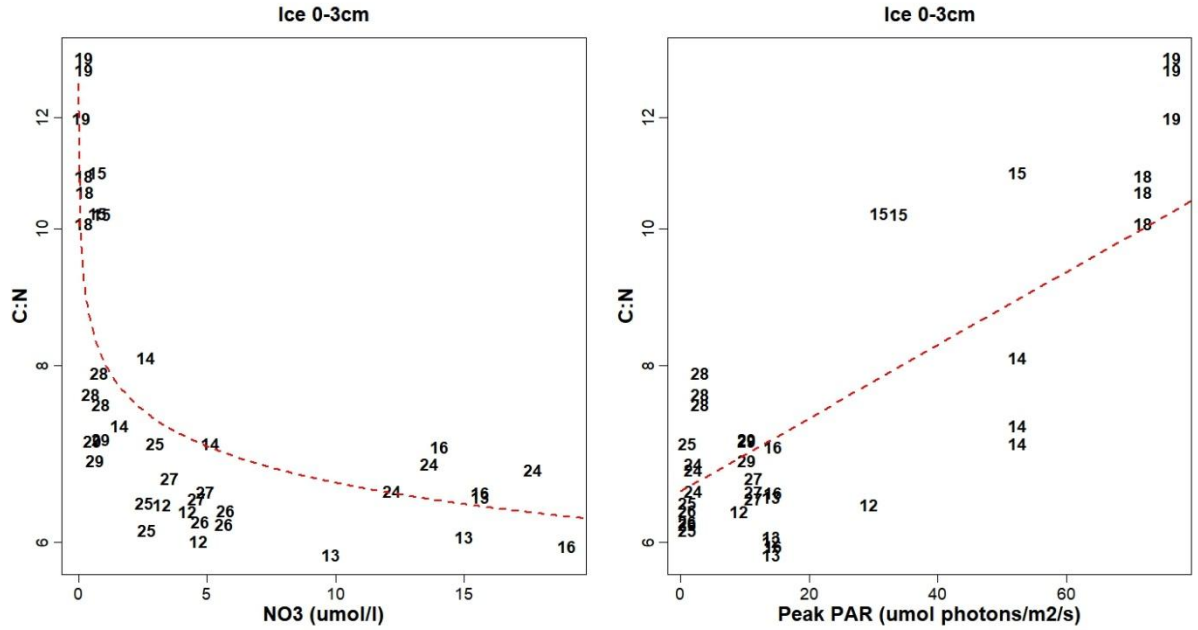

Figure 10. Scatterplots showing the C:N ratio versus nitrate (left panel) and light (right panel) for the sympagic samples from April and May. The numbers code for snow depth and sample, with the first digit coding for either low (1) or high (2) snow and the second digit coding for the sample (2=7th of April/MS, 3=8th of April/vMF1, 4=23rd of April/MS, 5=26th of April/vMF2, 16=28th of April/IS, 26=28th of April/IM, 7=29th of April/MS, 18=30th of April/vMF2, 28=30th of April/vMF1 and 9= 2nd of May/MS. The red line in the left panel is the function: ln(C:N) = 2.086 - 0.0858 ln(NO3), p<0.001. The red line in the right panel shows the relationship: C:N = exp(1.8746 + 0.005974*Peak PAR), p<0.0001.

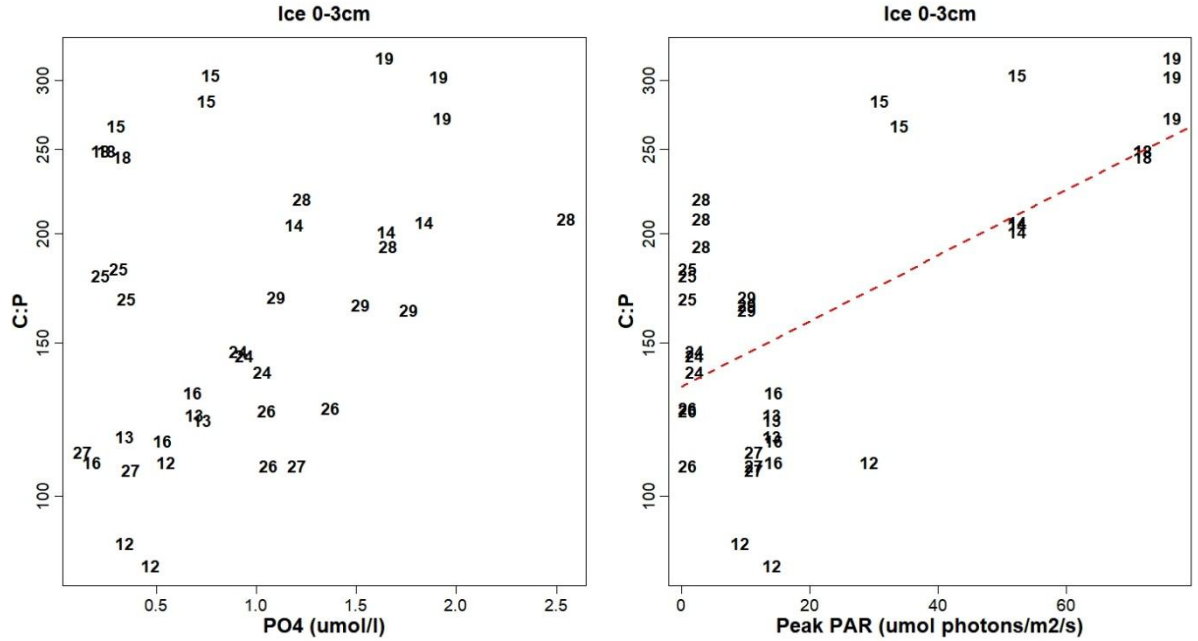

Figure 11. Scatterplots showing the C:P ratio versus phosphate (left panel) and light (right panel) for the sympagic samples from April and May. The numbers code for snow depth and sample, with the first digit coding for either low (1) or high (2) snow and the second digit coding for the sample (2=7th of April/MS, 3=8th of April/vMF1, 4=23rd of April/MS, 5=26th of April/vMF2, 16=28th of April/IS, 26=28th of April/IM, 7=29th of April/MS, 18=30th of April/vMF2, 28=30th of April/vMF1 and 9= 2nd of May/MS. The red line in the right panel shows the relationship: C:P = exp(4.8931 + 0.008714*Peak PAR), p<0.001.

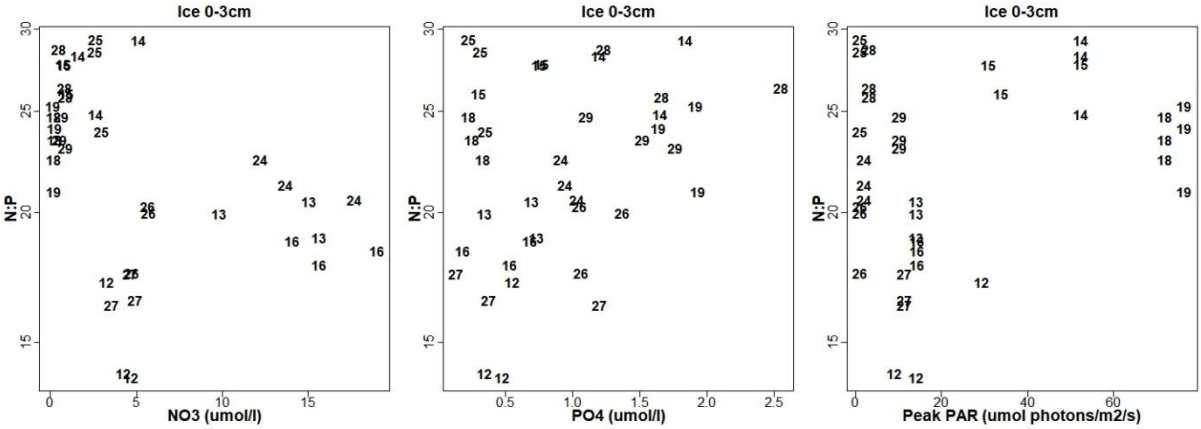

Figure 12. Scatterplots showing the N:P ratio versus nitrate (left panel), phosphate (middle panel) and light (right panel) for the sympagic samples from April and May. The numbers code for snow depth and sample, with the first digit coding for either low (1) or high (2) snow and the second digit coding for the sample (2=7th of April/MS, 3=8th of April/vMF1, 4=23rd of April/MS, 5=26th of April/vMF2, 16=28th of April/IS, 26=28th of April/IM, 7=29th of April/MS, 18=30th of April/vMF2, 28=30th of April/vMF1 and 9= 2nd of May/MS.

Discussion

Due to the nature of their respective habitats, phytoplankton and ice algae experience different light and nutrient regimes. Phytoplankton continuously circulates within the mixed layer, and as a result it is subjected to a range of different light levels on short timescales, which makes it hard to adapt to one specific light level. Pelagic algae have however a large reservoir of nutrients to their disposal, and typically only experience nutrient limitation when the entire reservoir is used up after the spring bloom. Ice algae on the other hand experience a somewhat opposite regime. They have a fixed position, and thus their light climate is relatively constant making light acclimation possible. Nutrients can be limiting for ice algae during their entire growing season, since they depend on a continuous exchange with the underlying water column. Since sea ice acts as a lid largely preventing gas exchange with the atmosphere, carbon limitation can also affect the growth of sympagic algae. These different habitats with their respective regimes have the potential to influence the elemental composition of the primary producers in different ways.
The stoichiometric ratios of pelagic as well as sympagic particulate organic matter showed a wide range of variability on both spatial and temporal scales. This is not unexpected, given the variations in light and nutrient availability over the course of the sampling period and between stations.

Sympagic results

The bulk of the ice algal biomass was found in the bottom three cm of the ice, where nutrients still get mixed into the ice by the action of tidal movements and currents (Cota, Prinsenberg et al. 1987). In contrast to their similar vertical position within the ice, on a spatial scale the ice algae were subject to strong differences in the amount of PAR they received. These differences were mainly caused by snow drifts formed by wind action (Mundy, Barber et al. 2005), which resulted in low (0-5 cm) and high (20-30 cm) snow areas. The timing of sea ice formation was also of influence at vMF2, as the late sea ice formation at that location prevented the accumulation of snow. Sympagic chlorophyll a concentrations dropped faster in areas with a low snow cover, because of two reasons. Firstly, the lack of thermal insulation facilitated the melting of the ice, releasing the sympagic algae into the water column (Mundy, Gosselin et al. 2014). Secondly, the abundance of light reduced the need for chlorophyll a in individual cells (Sterner, Elser 2002), (Arrigo 2004), as evidenced by the increases in POC:Chl a ratios.

The ice algae in the lower 0-3 cm of the ice showed clear signs of light acclimation, as evidenced by the positive linear relationship of the C:N and C:P ratios with the available PAR levels. Despite that in the 3-10 cm sections the variations in incoming irradiance must have been similar to the 0-3 cm sections, in the upper sections of the ice, this relationship was absent. A proximate explanation for this could be that the stoichiometric ratios in the 3-10 cm sections were most of the times near their upper limit, although higher values have been reported elsewhere (Niemi, Michel 2015), (Frigstad, Andersen et al. 2014). Higher up in the ice, temperature can become an important factor influencing algal stoichiometry. Ice temperatures in the 3-10 cm sections were typically lower than those in the 0-3 cm section, resulting in higher brine salinities. High salinities have been reported to negatively impact photosynthetic activity and algal growth rates (Grant, Horner 1976), (Palmisano, SooHoo et al. 1987). Reduced photosynthetic activity and growth rate have been found to coincide with changes in stoichiometric ratios (Leu, Falk-Petersen et al. 2007), (Sterner, Elser 2002).

Next to light availability, nitrate concentrations were also found to impact C:N ratios. The sharp increase in C:N ratios at nitrate concentrations below 3 µmol/l was best modelled using a log/log dependence, similar to Galbraith (Galbraith, Martiny 2015). Campbell (Campbell, Mundy et al. 2016) also found nitrogen limitation to be an important factor governing the stoichiometry of ice algae. One has to keep in mind however, that nutrient concentrations cannot be completely decoupled from light availability, as indirectly, light causes the drawdown of nutrients. In the field, the communities with the highest C:N ratios received the most light and had the lowest nitrate concentrations.
The potential shifts in species composition across the seasons and along the transect are not known for the present study, but phylogenetic effects on stoichiometric ratios can be of the same magnitude as phenotypic effects (Finkel, Quigg et al. 2006), (Ho, Quigg et al. 2003).

Pelagic results

The phytoplankton bloom at vMF1 developed in clearly stratified water, when it was still ice covered. The maximum chlorophyll a concentration was very close to the surface, whereas the phytoplankton biomass was distributed more evenly at the deeper stations in the outer basin of Van Mijenfjorden (VMF5), and in Bellsund (VMF9), where the water column did not show clear signs of stratification. Nutrients were depleted rapidly (within 2 weeks) in the stratified bloom under the sea ice, but stayed at higher levels outside.
Until recently pelagic blooms in seasonally ice covered waters were thought to occur mostly after ice break up ((Leu, Søreide et al. 2011) and references therein), but recently there has been an increasing amount of evidence that these under ice phytoplankton blooms are a common phenomenon (Arrigo, Perovich et al. 2012), (Mundy, Gosselin et al. 2014), (Assmy, FernÃ¡ndez-MÃ©ndez et al. 2017). The under ice bloom found at vMF1 can be added to this list. Similar to the study by Mundy (Mundy, Gosselin et al. 2014), the presence of the pelagic bloom can be partly attributed to the onset of the snowmelt, reducing the albedo of the snow cover and increasing the transmittance of light. Part of the ice algae had sloughed from the ice, but contrary to the study by Mundy, this could not be called a majority. At vMF1, sympagic chlorophyll a had only reduced by 40 percent compared to early April, and the pelagic and sympagic blooms more or less coincided, instead of being at least a week apart as reported by Mundy. The pelagic bloom coincided with a drop in nitrate and phosphate concentrations, so the sloughing of ice algae was not the main cause for the pelagic chlorophyll a concentrations, as proposed by others (Weydmann, Søreide et al. 2013).

The pelagic bloom at vMF1 did not experience high irradiances due to the shading effect of the snow and ice covering the water. Similarly, the phytoplankton at vMF5 and vMF9 were mixed down to up to one hundred meters of water depth, so it is no surprise that no clear effects of high irradiance on stoichiometric ratio were found.

Pelagic samples fell apart into two groups. One consisted of early season and bottom samples with high C:N/C:P ratios coupled to high nutrient concentrations. The other consisted of bloom samples with predominantly lower stoichiometric ratios (C:N < 8, C:P < 180) and lower nutrient concentrations (nitrate < 6 µmol/l, phosphate < 0.4 µmol/l). Because these two groups had very contrasting properties, there was a very strong positive relationship between stoichiometric ratios and nutrients, when performing analysis on the entire sample set. This can be attributed to the high fraction of non algal material in the early season/bottom samples.
Only when taking a subset consisting solely of the open water samples from April and June a negative

dependence between nitrate and stoichiometric ratios was found (data not shown).

Soil age is an important factor in the sequestration of phosphorus, and the young age, in geological terms, of the soils on Svalbard facilitates the transport of phosphorus towards the estuaries (Elser, Bracken et al. 2007). The episodic release of large quantities of melt water by glaciers is associated with simultaneous of large amounts of phosphorus (Hodson, Mumford et al. 2004). Svalbard is covered for 60 percent with glaciers, and there are in excess of 20 glaciers that directly or indirectly discharge in van Mijenfjorden. The semiclosed nature of van Mijenfjorden limits the exchange with water from outside the fjord. Arctic riverine phosphorus export as well as glacial phosphorus export are among the highest reported fluxes (Hawkings, Wadham et al. 2016). Although no direct measurements of terrestrial phosphorus fluxes were taken for this study, the nature of the system studied is likely to preclude phosphorus limitation.

Nitrogen limitation, on the other hand, is a widespread phenomenon in the oceans (Elser, Bracken et al. 2007) and given the considerations above, nitrate availability is most likely also the main factor controlling the primary production in van Mijenfjorden.

The relatively high nitrate and phosphate concentrations combined with relatively low chlorophyll a concentrations in June at vMF5, contrasted with the relatively low nutrient and high chlorophyll a concentrations at vMF9 at the same time. This difference seems to indicate different types of control at these locations (i.e. top down vs bottom up). A previous study at the same location reported similar conditions and identified grazing by zooplankton as the likely factor regulating the phytoplankton abundance in summer within the fjord (Eilertsen, Taasen et al. 1989).

Seasonality

A major sampling bias occurs when collecting microalgal communities as filter samples, because the sampling method makes it impossible to distinguish between live algal cells and detrital material. Due to the strong seasonality of algal growth in the Arctic, the contribution of algal matter to the total pool of particulate organic matter (POM) varied strongly across the seasons. This was evident in both pelagic and sympagic POM. In January and March when chlorophyll a concentrations were low, POC:Chl a ratios were between 600 and 2600, considerably outside the range of 40 to 200 typical of algae as reported by Harris (Harris 2012). Similar high POC:Chl a ratios have also been reported from the Canadian Arctic Archipelago, with maximum ratios even an order of magnitude higher than the current study (Niemi, Michel 2015). During these winter months, stoichiometric ratios of POM are not indicative of algal stoichiometry, but are more likely to be heavily influenced by detritus. The selective decomposition of detritus can also explain the increase in nutrient concentrations and C:N and C:P ratios during winter.

With the return of the light, algae quickly started to dominate the sympagic POM pool as evidenced by the sudden decrease in POC:Chl a ratios in early April. The POC:Chl a ratios of 25-35 during the spring bloom are similar to the lower values reported by Nozais (33-89) (Nozais, Gosselin et al. 2001),Michel (27-67) (Michel, Legendre et al. 1996), Campbell (29-235) (Campbell, Mundy et al. 2016) and the meta study by Leu (20-45) (Leu, Mundy et al. 2015). In this study uncorrected chlorophyll a values were used, so reported chlorophyll a concentrations are likely overestimations. For the April spring bloom, using the data for which the correction was made, this over estimation is just under a factor of 2 (data not shown). When accounting for this, the new data still fit well with the previously reported spring bloom values.

Methodological differences

The observation that incoming irradiance was not a factor determining the stoichiometry of pelagic

algae, can be largely attributed to the physical properties of the water columns at the different sampling days and stations. Apart from the sampling at vMF9, and to a lesser degree vMF5, in June, the water column was generally well mixed, which resulted in algae being subjected to a variety of different light levels. This would have prevented algae of adapting to a specific light level, thus making it impossible to assess the contribution of different light levels to differences in stoichiometric ratios.

In contrast to pelagic algae, sympagic algae experienced relatively constant light levels. As a result, the natural variations in snow depth made it possible to assess the influence of light on stoichiometry. Thus, by nature of their different habitats, one can expect the stoichiometry of sympagic algae to be more governed by irradiance levels than that of pelagic algae.

One of the advantages of sea ice found is this study is that it makes the study of an in situ ecosystem dominated by algae possible over a longer period of time. In contrast to the pelagic community, the sympagic community stayed dominated by ice algae throughout the growing season, as evidenced by the relatively stable POC:Chl a ratios. Despite the presence of meiofauna in the ice, grazing occurs predominantly by copepods. In seston samples it is hard to differentiate between algae, zooplankton and detritus. The sampling method of ice coring excludes anything that is not frozen in the ice. Terrestrial material that is exported into the fjord when it gets warmer is therefore not obscuring stoichiometric signals from autotrophic responses to changing light and nutrient conditions. Similarly, a high grazer density is mainly affecting the algal biomass, but since copepods are not attached to the ice, their inclusion in ice samples is limited.

Conclusion

The differences in habitat of sympagic and pelagic algae were reflected in differences in the main drivers found to influence stoichiometry. Light and nutrients are both essential for autotrophs, however adaptation to light required the relatively stable conditions found in the ice. Another aspects that sets sea ice apart from the pelagic realm, is that it remains dominated by autotrophs over an extended period of time. As a result, ice based sampling can potentially offer insights into autotrophic processes that are hard to get from bulk seston, where autotrophic signals rapidly get obscured by heterotrophic and detrital ones. Although ice sampling can be logistically demanding, especially in the light of climatic changes, continued efforts into studying sympagic system are of prime importance.

Acknowledgements

None of this would have been possible without the help and guidance of Eva. I will never understand where she found all the patience needed to guide me, but I'm glad she did. I would further like to thank Katja for supporting me, and for signing too many forms. Ane for being unable to stress and being the best teammate during fieldwork. Michael for his much needed advice on the statistics. And for fear of forgetting someone, all the other fabulous team members involved in the project.

Literature

ARRIGO, K.R., 2013. The changing Arctic Ocean. *Elem Sci Anth,* **1**.

ARRIGO, K.R., 2004. Marine microorganisms and global nutrient cycles. *Nature,* **437**(7057), pp. 349.

ARRIGO, K.R. and VAN DIJKEN, G.L., 2011. Secular trends in Arctic Ocean net primary production. *Journal of Geophysical Research: Oceans,* **116**(C9),.

ARRIGO, K.R., PEROVICH, D.K., PICKART, R.S., BROWN, Z.W., VAN DIJKEN, G.L., LOWRY, K.E., MILLS, M.M., PALMER, M.A., BALCH, W.M., BAHR, F., BATES, N.R., BENITEZ-NELSON, C., BOWLER, B., BROWNLEE, E., EHN, J.K., FREY, K.E., GARLEY, R., LANEY, S.R., LUBELCZYK, L., MATHIS, J., MATSUOKA, A., MITCHELL, B.G., MOORE, G.W., ORTEGA-RETUERTA, E., PAL, S., POLASHENSKI, C.M., REYNOLDS, R.A., SCHIEBER, B., SOSIK, H.M., STEPHENS, M. and SWIFT, J.H., 2012. Massive phytoplankton blooms under Arctic sea ice. *Science (New York, N.Y.),* **336**(6087), pp. 1408.

ASSMY, P., FERNÃ¡NDEZ-MÃ©NDEZ, M., DUARTE, P., MEYER, A., RANDELHOFF, A., MUNDY, C.J., OLSEN, L.M., KAUKO, H.M., BAILEY, A., CHIERICI, M., COHEN, L., DOULGERIS, A.P., EHN, J.K., FRANSSON, A., GERLAND, S., HOP, H., HUDSON, S.R., HUGHES, N., ITKIN, P., JOHNSEN, G., KING, J.A., KOCH, B.P., KOENIG, Z., KWASNIEWSKI, S., LANEY, S.R., NICOLAUS, M., PAVLOV, A.K., POLASHENSKI, C.M., PROVOST, C., RÃ¶SEL, A., SANDBU, M., SPREEN, G., SMEDSRUD, L.H., SUNDFJORD, A., TASKJELLE, T., TATAREK, A., WIKTOR, J., WAGNER, P.M., WOLD, A., STEEN, H. and GRANSKOG, M.A., 2017. Leads in Arctic pack ice enable early phytoplankton blooms below snow-covered sea ice. *Scientific Reports,* **7**, pp. 40850.

BARTSCH, A., 1989. Sea ice algae of the Weddell Sea(Antarctica): Species composition, biomass, and ecophysiology of selected species. *Berichte zur Polarforschung/Reports on polar research.1989.,* .

CAMPBELL, K., MUNDY, C., BARBER, D. and GOSSELIN, M., 2015. Characterizing the sea ice algae chlorophyll a–snow depth relationship over Arctic spring melt using transmitted irradiance. *Journal of Marine Systems,* **147**, pp. 76-84.

CAMPBELL, K., MUNDY, C.J., LANDY, J.C., DELAFORGE, A., MICHEL, C. and RYSGAARD, S., 2016. *Community dynamics of bottom-ice algae in Dease Strait of the Canadian Arctic.*

COTA, G., PRINSENBERG, S., BENNETT, E., LODER, J., LEWIS, M., ANNING, J., WATSON, N. and HARRIS, L., 1987. Nutrient fluxes during extended blooms of Arctic ice algae. *Journal of Geophysical Research: Oceans,* **92**(C2), pp. 1951-1962.

COX, G.F. and WEEKS, W.F., 1983. Equations for determining the gas and brine volumes in sea-ice samples. *Journal of Glaciology,* **29**(102), pp. 306-316.

DALY, K.L., WALLACE, D.W., SMITH, W.O., SKOOG, A., LARA, R., GOSSELIN, M., FALCK, E. and YAGER, P.L., 1999. Non-Redfield carbon and nitrogen cycling in the Arctic: Effects of ecosystem structure and dynamics. *Journal of Geophysical Research: Oceans,* **104**(C2), pp. 3185-3199.

EICKEN, H., 1992. The role of sea ice in structuring Antarctic ecosystems. *Weddell Sea Ecology.* Springer, pp. 3-13.

EILERTSEN, H.C., TAASEN, J.P. and WESIAWSKI, J.M., 1989. Phytoplankton studies in the fjords of West Spitzbergen: physical environment and production in spring and summer. *Journal of Plankton Research,* **11**(6), pp. 1245-1260.

ELSER, J.J., BRACKEN, M.E., CLELAND, E.E., GRUNER, D.S., STANLEY, H.W., HELMUT, H., NGAI, J.T., SEABLOOM, E.W., SHURIN, J.B. and SMITH, J.E., 2007. Global analysis of nitrogen and phosphorus limitation of primary producers in freshwater, marine and terrestrial ecosystems. *Ecology Letters,* **10**(12), pp. 1135-1142.

FALKOWSKI, P.G., 2000. Rationalizing elemental ratios in unicellular algae. *Journal of Phycology,* **36**(1), pp. 3-6.

FINKEL, Z., QUIGG, A., RAVEN, J., REINFELDER, J., SCHOFIELD, O. and FALKOWSKI, P., 2006. Irradiance and the elemental stoichiometry of marine phytoplankton. *Limnology and Oceanography,* **51**(6), pp. 2690-2701.

FRIGSTAD, H., ANDERSEN, T., BELLERBY, R.G., SILYAKOVA, A. and HESSEN, D.O., 2014. Variation in the seston C: N ratio of the Arctic Ocean and pan-Arctic shelves. *Journal of Marine Systems,* **129**, pp. 214-223.

GALBRAITH, E.D. and MARTINY, A.C., 2015. A simple nutrient-dependence mechanism for predicting the stoichiometry of marine ecosystems. *Proceedings of the National Academy of Sciences of the United States of America,* **112**(27), pp. 8199-8204.

GOSSELIN, M., LEVASSEUR, M., WHEELER, P.A., HORNER, R.A. and BOOTH, B.C., 1997. New measurements of phytoplankton and ice algal production in the Arctic Ocean. *Deep Sea Research Part II: Topical Studies in Oceanography,* **44**(8), pp. 1623-1644.

GRANT, W. and HORNER, R.A., 1976. Growth responses to salinity variation in four Arctic ice diatoms. *Journal of Phycology,* **12**(2), pp. 180-185.

HARRIS, G., 2012. *Phytoplankton ecology: structure, function and fluctuation.* Springer Science & Business Media.

HARTMANN, D.L., KLEIN TANK, A.M.G., RUSTICUCCI, M., ALEXANDER, L.V., BRÖNNIMANN, S., CHARABI, Y., DENTENER, F.J., DLUGOKENCKY, E.J., EASTERLING, D.R., KAPLAN, A., SODEN, B.J., THORNE, P.W., WILD, M. and ZHAI, P.M., 2013. Observations: Atmosphere and Surface. *Climate Change 2013: The Physical Science Basis.* Cambridge, United Kingdom: Cambridge University Press, .

HAWKINGS, J., WADHAM, J., TRANTER, M., TELLING, J., BAGSHAW, E., BEATON, A., SIMMONS, S., CHANDLER, D., TEDSTONE, A. and NIENOW, P., 2016. The Greenland Ice Sheet as a hot spot of phosphorus weathering and export in the Arctic. *Global Biogeochemical Cycles,* **30**(2), pp. 191-210.

HESSEN, D.O., LEU, E., FÆRØVIG, P.J. and PETERSEN, S.F., 2008. Light and spectral properties as determinants of C: N: P-ratios in phytoplankton. *Deep Sea Research Part II: Topical Studies in Oceanography,* **55**(20-21), pp. 2169-2175.

HO, T., QUIGG, A., FINKEL, Z.V., MILLIGAN, A.J., WYMAN, K., FALKOWSKI, P.G. and MOREL, F.M., 2003. The elemental composition of some marine phytoplankton. *Journal of Phycology,* **39**(6), pp. 1145-1159.

HODSON, A., MUMFORD, P. and LISTER, D., 2004. Suspended sediment and phosphorus in proglacial rivers: bioavailability and potential impacts upon the P status of ice-marginal receiving waters. *Hydrological Processes,* **18**(13), pp. 2409-2422.

JÓNASDÓTTIR, S., GUDFINNSSON, H., GISLASON, A. and ASTTHORSSON, O., 2002. Diet composition and quality for Calanus finmarchicus egg production and hatching success off south-west Iceland. *Marine Biology,* **140**(6), pp. 1195-1206.

KOTTMEIER, S.T. and SULLIVAN, C.W., 1988. Sea ice microbial communities (SIMCO). *Polar Biology,* **8**(4), pp. 293-304.

LEU, E., MUNDY, C., ASSMY, P., CAMPBELL, K., GABRIELSEN, T., GOSSELIN, M., JUUL-PEDERSEN, T. and GRADINGER, R., 2015. Arctic spring awakening–Steering principles behind the phenology of vernal ice algal blooms. *Progress in Oceanography,* **139**, pp. 151-170.

LEU, E., SØREIDE, J., HESSEN, D., FALK-PETERSEN, S. and BERGE, J., 2011. Consequences of changing sea-ice cover for primary and secondary producers in the European Arctic shelf seas: timing, quantity, and quality. *Progress in Oceanography,* **90**(1-4), pp. 18-32.

LEU, E., FALK-PETERSEN, S. and HESSEN, D.O., 2007. Ultraviolet radiation negatively affects growth but not food quality of arctic diatoms. *Limnology and Oceanography,* **52**(2), pp. 787-797.

MCMINN, A., SKERRATT, J., TRULL, T., ASHWORTH, C. and LIZOTTE, M., 1999. Nutrient stress gradient in the bottom 5 cm of fast ice, McMurdo Sound, Antarctica. *Polar Biology,* **21**(4), pp. 220-227.

MICHEL, C., INGRAM, R. and HARRIS, L., 2006. Variability in oceanographic and ecological processes in the Canadian Arctic Archipelago. *Progress in Oceanography,* **71**(2-4), pp. 379-401.

MICHEL, C., LEGENDRE, L., INGRAM, R., GOSSELIN, M. and LEVASSEUR, M., 1996. Carbon budget of sea-ice algae in spring: Evidence of a significant transfer to zooplankton grazers. *Journal of Geophysical Research: Oceans,* **101**(C8), pp. 18345-18360.

MUNDY, C., BARBER, D. and MICHEL, C., 2005. Variability of snow and ice thermal, physical and optical properties pertinent to sea ice algae biomass during spring. *Journal of Marine Systems,* **58**(3-4), pp. 107-120.

MUNDY, C., GOSSELIN, M., GRATTON, Y., BROWN, K., GALINDO, V., CAMPBELL, K., LEVASSEUR, M., BARBER, D., PAPAKYRIAKOU, T. and BÉLANGER, S., 2014. Role of environmental factors on phytoplankton bloom initiation under landfast sea ice in Resolute Passage, Canada. *Marine Ecology Progress Series,* **497**, pp. 39-49.

NIEMI, A. and MICHEL, C., 2015. Temporal and spatial variability in sea-ice carbon: nitrogen ratios on Canadian Arctic shelves. *Elem Sci Anth,* **3**.

NIEMI, A., MICHEL, C., HILLE, K. and POULIN, M., 2011. Protist assemblages in winter sea ice: setting the stage for the spring ice algal bloom. *Polar Biology,* **34**(12), pp. 1803-1817.

NOTZ, D. and STROEVE, J., 2016. Observed Arctic sea-ice loss directly follows anthropogenic CO2 emission. *Science (New York, N.Y.),* **354**(6313), pp. 747-750.

NOZAIS, C., GOSSELIN, M., MICHEL, C. and TITA, G., 2001. Abundance, biomass, composition and grazing impact of the sea-ice meiofauna in the North Water, northern Baffin Bay. *Marine Ecology Progress Series,* **217**, pp. 235-250.

PABI, S., VAN DIJKEN, G.L. and ARRIGO, K.R., 2008. Primary production in the Arctic Ocean, 1998–2006. *Journal of Geophysical Research: Oceans,* **113**(C8),.

PALMISANO, A., SOOHOO, J.B. and SULLIVAN, C., 1987. Effects of four environmental variables on photosynthesis-irradiance relationships in Antarctic sea-ice microalgae. *Marine Biology,* **94**(2), pp. 299-306.

PEROVICH, D.K. and RICHTER-MENGE, J.A., 2009. Loss of sea ice in the Arctic. *Annual Review of Marine Science,* **1**, pp. 417-441.

PERRETTE, M., YOOL, A., QUARTLY, G. and POPOVA, E., 2011. Near-ubiquity of ice-edge blooms in the Arctic. *Biogeosciences,* **8**(2), pp. 515-524.

PETERSON, B.J., HOLMES, R.M., MCCLELLAND, J.W., VOROSMARTY, C.J., LAMMERS, R.B., SHIKLOMANOV, A.I., SHIKLOMANOV, I.A. and RAHMSTORF, S., 2002. Increasing river discharge to the Arctic Ocean. *Science (New York, N.Y.),* **298**(5601), pp. 2171-2173.

REDFIELD, A.C., 1958. The biological control of chemical factors in the environment. *American Scientist,* **46**(3), pp. 230A-221.

SLAGSTAD, D., ELLINGSEN, I. and WASSMANN, P., 2011. Evaluating primary and secondary production in an Arctic Ocean void of summer sea ice: an experimental simulation approach. *Progress in Oceanography,* **90**(1-4), pp. 117-131.

SØREIDE, J.E., LEU, E., BERGE, J., GRAEVE, M. and FALK-PETERSEN, S., 2010. Timing of blooms, algal food quality and Calanus glacialis reproduction and growth in a changing Arctic. *Global Change Biology,* **16**(11), pp. 3154-3163.

STERNER, R.W., ANDERSEN, T., ELSER, J.J., HESSEN, D.O., HOOD, J.M., MCCAULEY, E. and URABE, J., 2008. Scale-dependent carbon: nitrogen: phosphorus seston stoichiometry in marine and freshwaters. *Limnology and Oceanography,* **53**(3), pp. 1169-1180.

STERNER, R.W. and ELSER, J.J., 2002. *Ecological stoichiometry: the biology of elements from molecules to the biosphere.* Princeton University Press.

THRANE, J., HESSEN, D.O. and ANDERSEN, T., 2016. The impact of irradiance on optimal and cellular nitrogen to phosphorus ratios in phytoplankton. *Ecology Letters,* **19**(8), pp. 880-888.

WASSMANN, P. and REIGSTAD, M., 2011. Future Arctic Ocean seasonal ice zones and implications for pelagic-benthic coupling. *Oceanography,* **24**(3), pp. 220-231.

WEYDMANN, A., SØREIDE, J.E., KWAŚNIEWSKI, S., LEU, E., FALK-PETERSEN, S. and BERGE, J., 2013. Ice-related seasonality in zooplankton community composition in a high Arctic fjord. *Journal of Plankton Research,* **35**(4), pp. 831-842.

ZHANG, Q., GRADINGER, R. and SPINDLER, M., 1999. Experimental study on the effect of salinity on growth rates of Arctic-sea-ice algae from the Greenland Sea. *Boreal Environment Research,* **4**, pp. 1-8.

Appendix A

The geographical coordinates of the different sampling stations.

Station name	**Latitude**	**Longitude**
IS (Inner Station)	77°53'4.00"N	16°43'51.00"E
IM (Intermediate Station)	77°51'56.00"N	16°42'19.00"E
MS (Main Station)	77°51'10.00"N	16°42'9.00"E
vMF1	77°49'52.00"N	16°37'10.00"E
vMF2	77°49'53.00"N	16°18'29.00"E
vMF3	77°47'38.00"N	15°48'30.00"E
vMF4	77°47'35.00"N	15°28'59.00"E
vMF5	77°46'1.00"N	15°2'39.00"E
vMF9	77°41'23.00"N	14°5'28.00"E

Appendix B

CTD casts from March, April and June at the ice edge, vMF5 and vMF9.

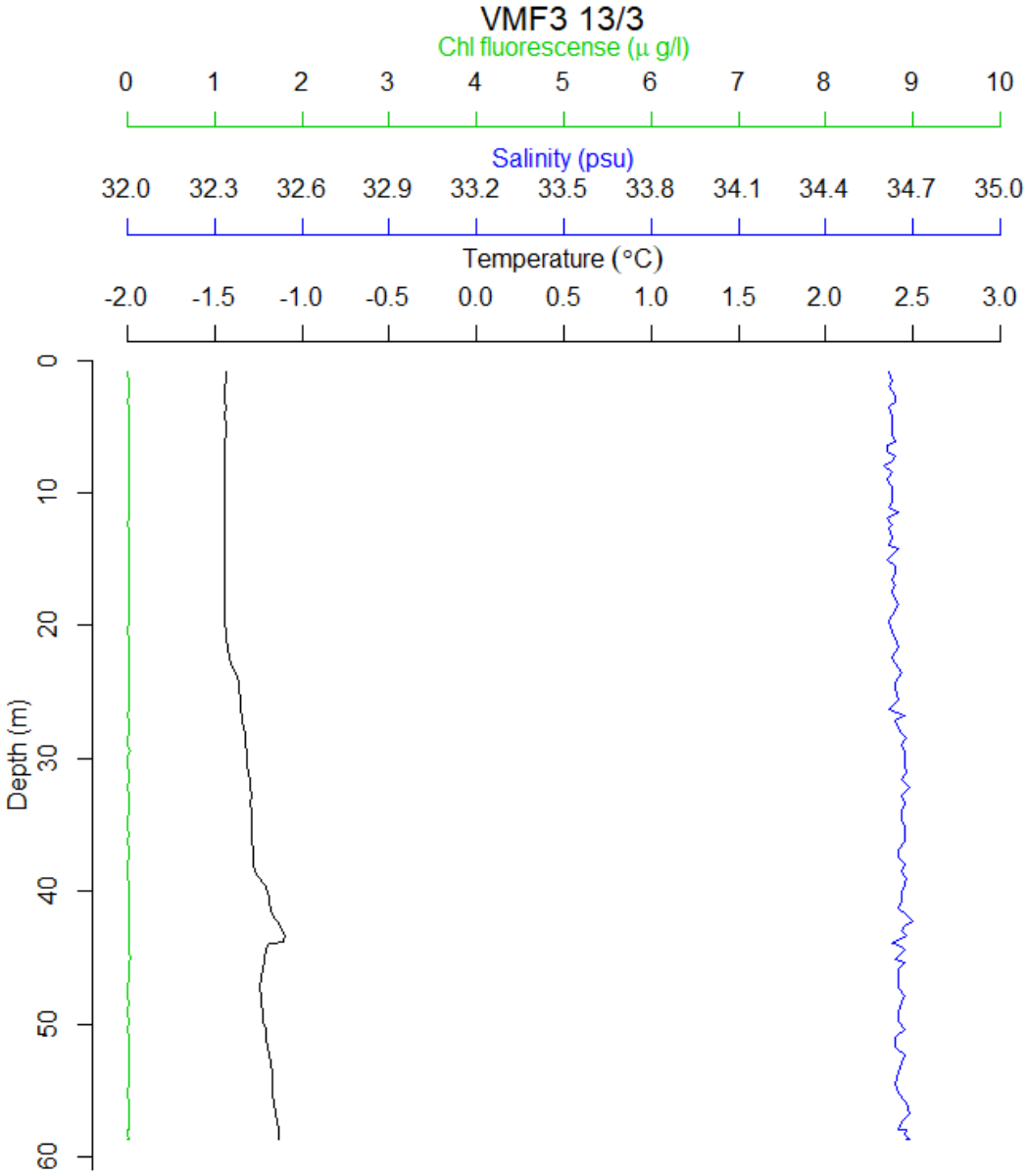

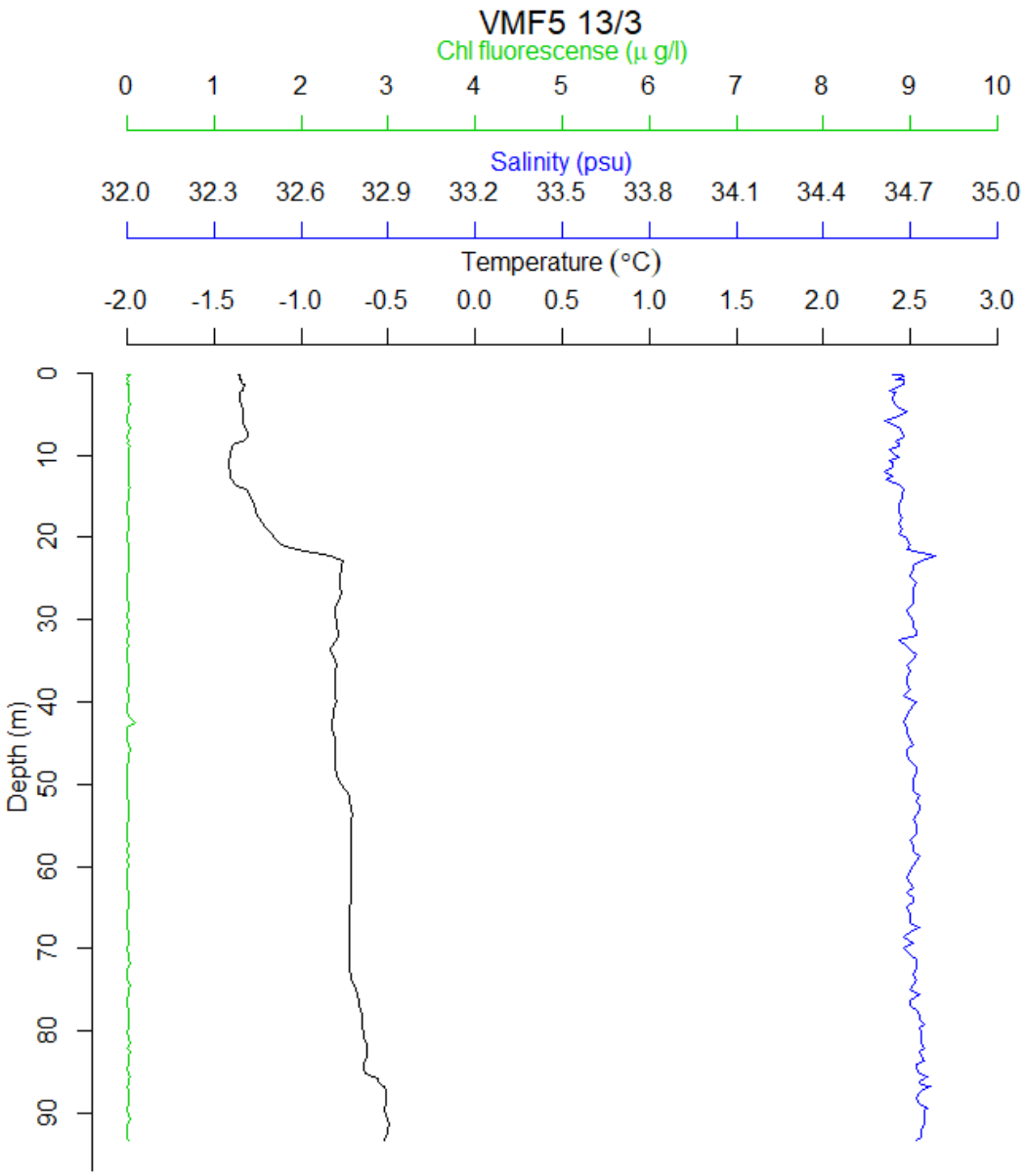
VMF5 13/3
Chl fluorescense (µ g/l)
0 1 2 3 4 5 6 7 8 9 10
Salinity (psu)
32.0 32.3 32.6 32.9 33.2 33.5 33.8 34.1 34.4 34.7 35.0
Temperature (°C)
-2.0 -1.5 -1.0 -0.5 0.0 0.5 1.0 1.5 2.0 2.5 3.0
Depth (m)
0 10 20 30 40 50 60 70 80 90

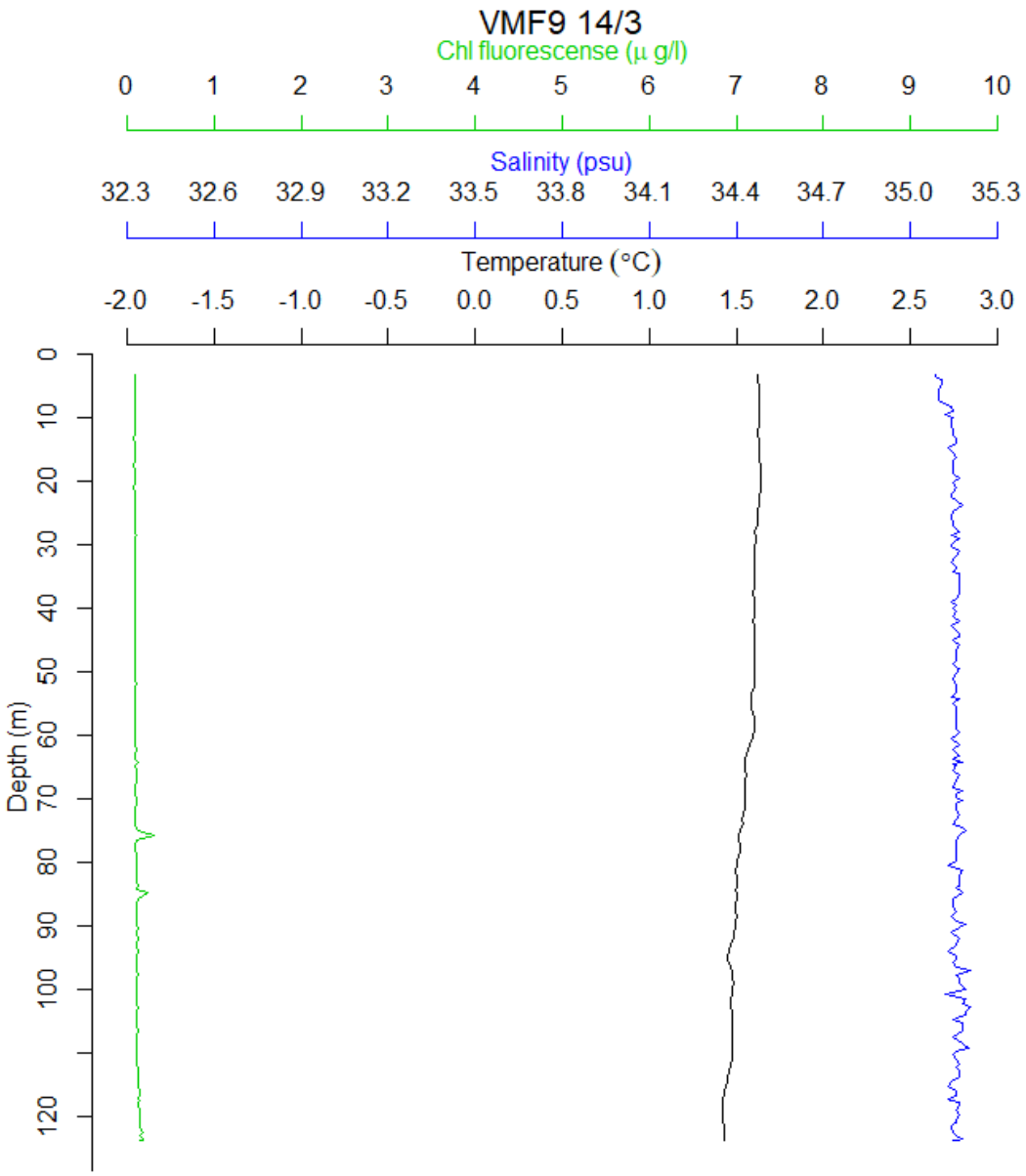
VMF9 14/3
Chl fluorescense (µ g/l)
0 1 2 3 4 5 6 7 8 9 10
Salinity (psu)
32.3 32.6 32.9 33.2 33.5 33.8 34.1 34.4 34.7 35.0 35.3
Temperature (°C)
-2.0 -1.5 -1.0 -0.5 0.0 0.5 1.0 1.5 2.0 2.5 3.0
Depth (m)
0 10 20 30 40 50 60 70 80 90 100 120

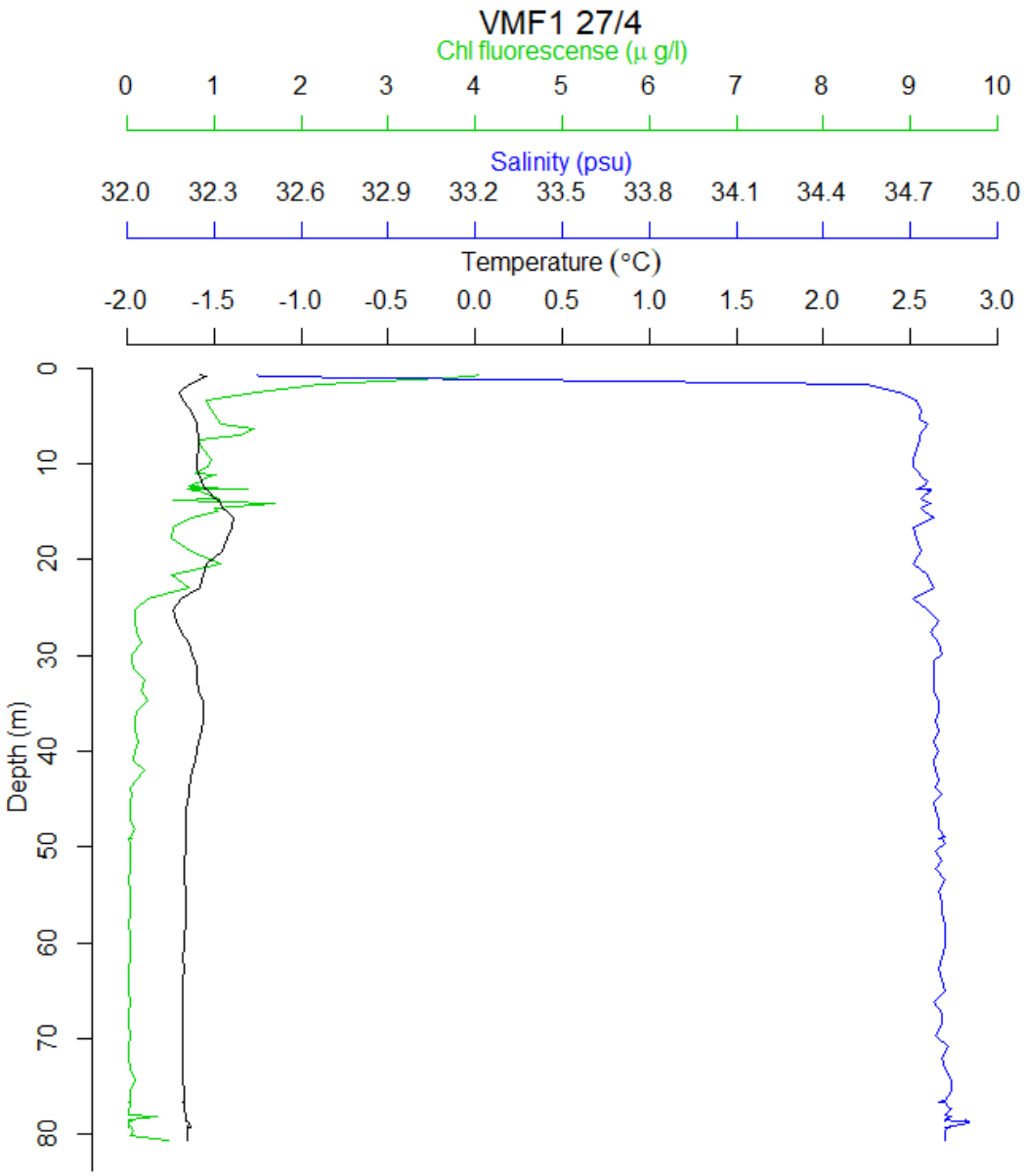
VMF1 27/4
Chl fluorescense (µ g/l)
0 1 2 3 4 5 6 7 8 9 10
Salinity (psu)
32.0 32.3 32.6 32.9 33.2 33.5 33.8 34.1 34.4 34.7 35.0
Temperature (°C)
-2.0 -1.5 -1.0 -0.5 0.0 0.5 1.0 1.5 2.0 2.5 3.0
Depth (m)
0 10 20 30 40 50 60 70 80

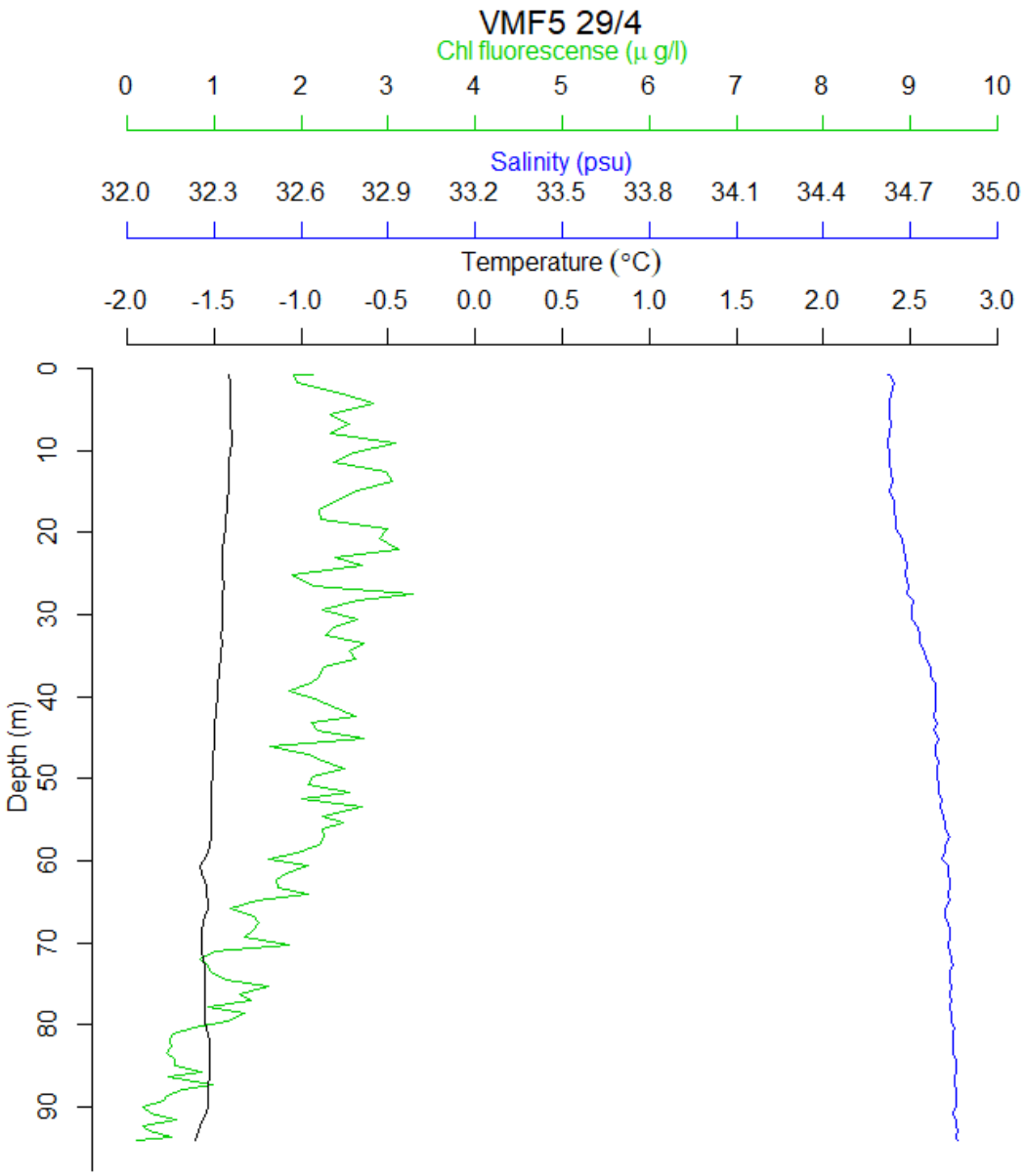
VMF5 29/4
Chl fluorescense (µ g/l)
0 1 2 3 4 5 6 7 8 9 10
Salinity (psu)
32.0 32.3 32.6 32.9 33.2 33.5 33.8 34.1 34.4 34.7 35.0
Temperature (°C)
-2.0 -1.5 -1.0 -0.5 0.0 0.5 1.0 1.5 2.0 2.5 3.0
Depth (m)
0 10 20 30 40 50 60 70 80 90

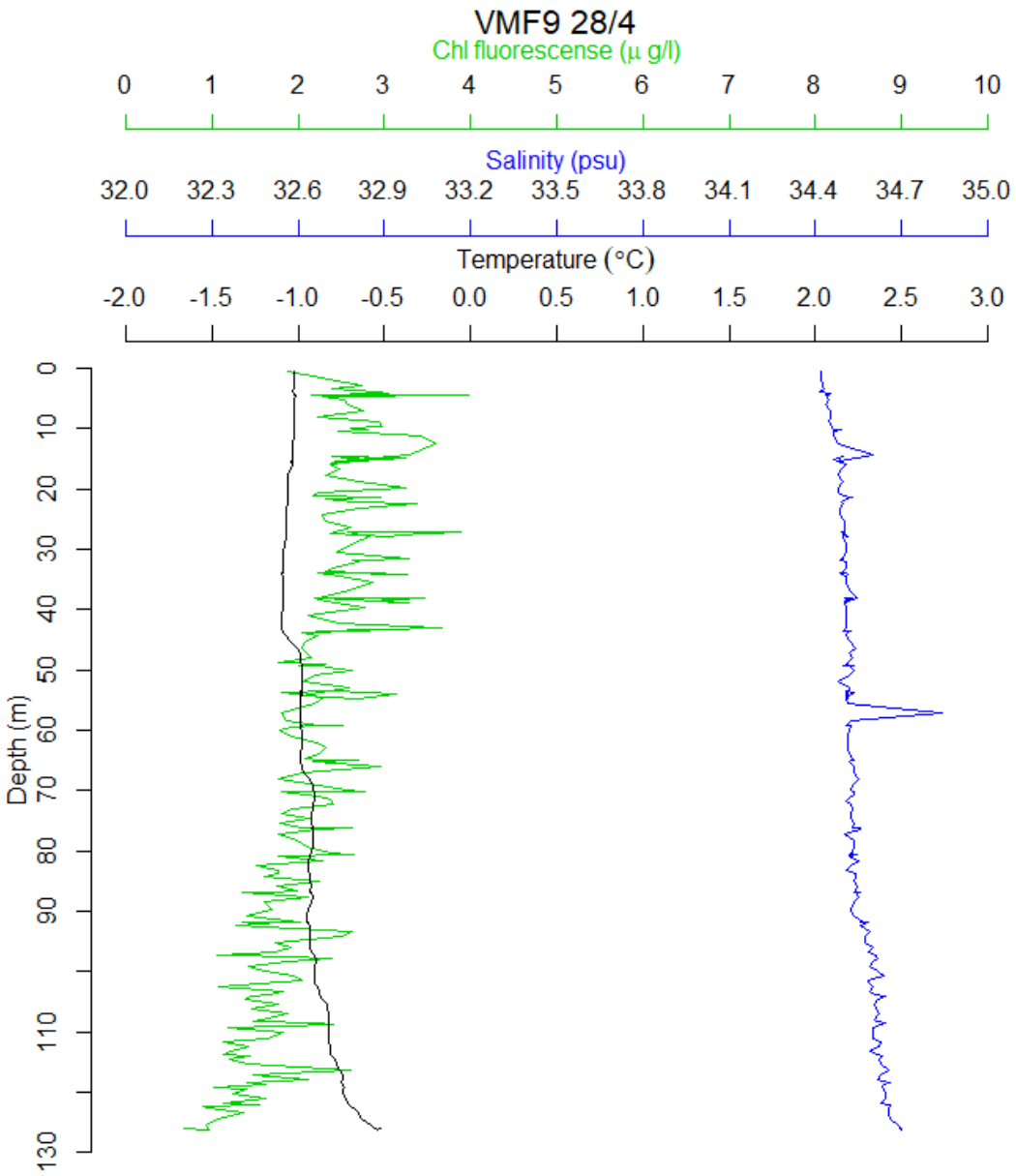
VMF9 28/4
Chl fluorescense (µ g/l)
0 1 2 3 4 5 6 7 8 9 10
Salinity (psu)
32.0 32.3 32.6 32.9 33.2 33.5 33.8 34.1 34.4 34.7 35.0
Temperature (°C)
-2.0 -1.5 -1.0 -0.5 0.0 0.5 1.0 1.5 2.0 2.5 3.0
Depth (m)
0 10 20 30 40 50 60 70 80 90 110 130

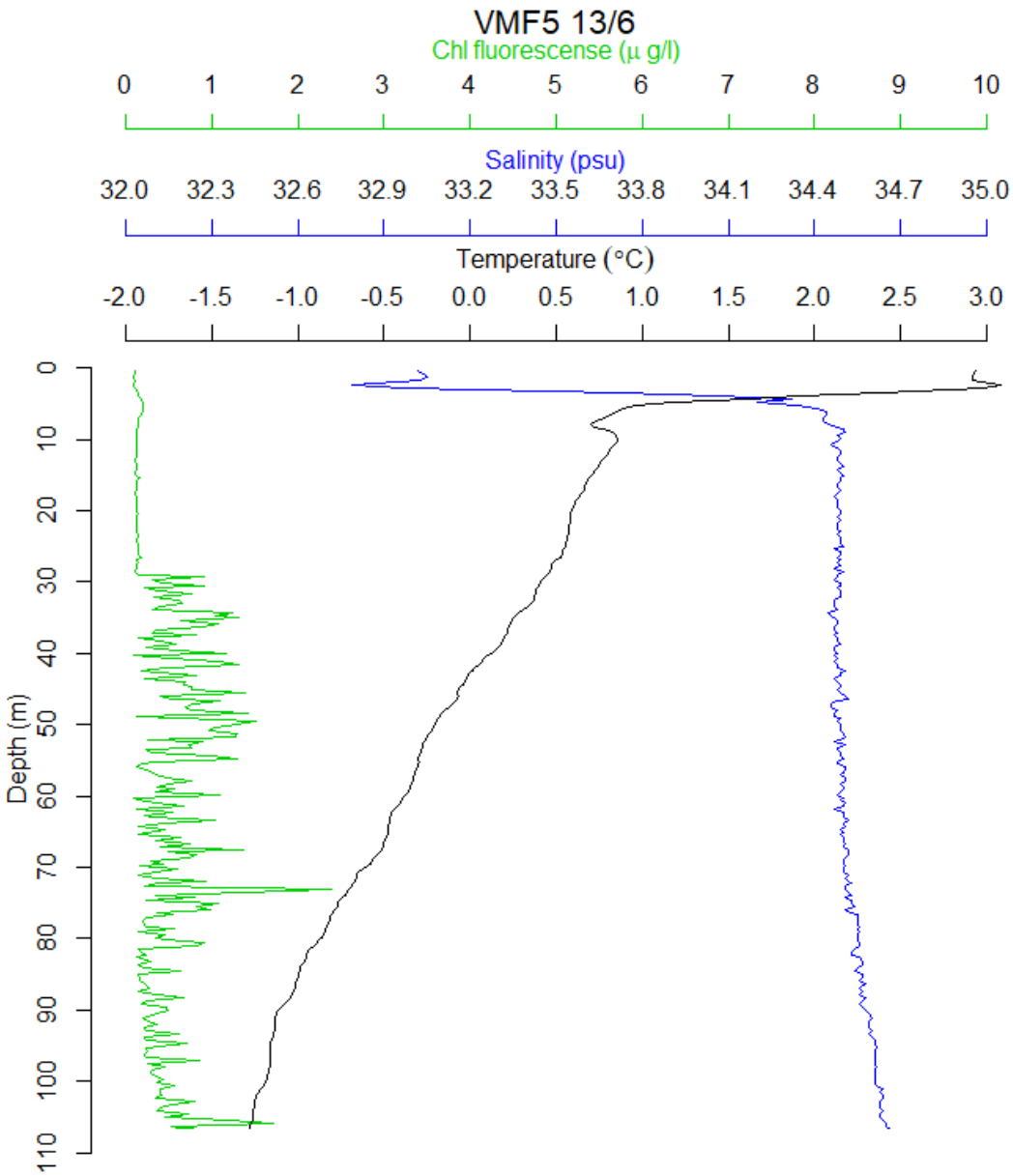
VMF5 13/6
Chl fluorescense (µ g/l)
0 1 2 3 4 5 6 7 8 9 10
Salinity (psu)
32.0 32.3 32.6 32.9 33.2 33.5 33.8 34.1 34.4 34.7 35.0
Temperature (°C)
-2.0 -1.5 -1.0 -0.5 0.0 0.5 1.0 1.5 2.0 2.5 3.0
Depth (m)
0 10 20 30 40 50 60 70 80 90 100 110

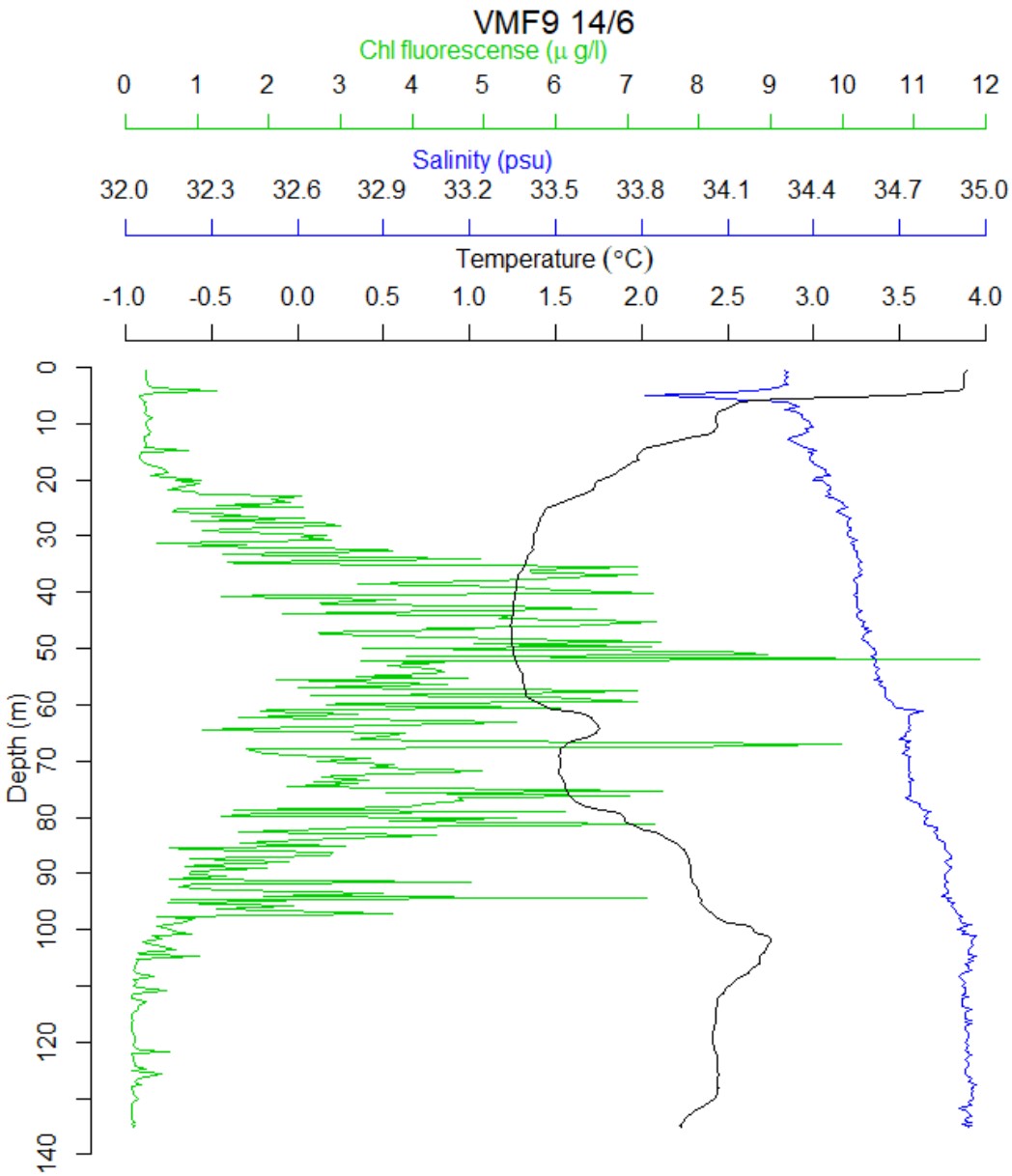
VMF9 14/6
Chl fluorescense (µ g/l)
0 1 2 3 4 5 6 7 8 9 10 11 12
Salinity (psu)
32.0 32.3 32.6 32.9 33.2 33.5 33.8 34.1 34.4 34.7 35.0
Temperature (°C)
-1.0 -0.5 0.0 0.5 1.0 1.5 2.0 2.5 3.0 3.5 4.0
Depth (m)
0 10 20 30 40 50 60 70 80 90 100 120 140